ADVANCING EARTH AND SPACE SCIENCE

JGR Earth Surface

RESEARCH ARTICLE
10.1029/2022JF006790

Effects of Sea-Level Rise on Dredging and Dredged Estuary Morphology

J. R. Cox[1], J. Lingbeek[1], S. A. H. Weisscher[1], and M. G. Kleinhans[1]

[1]Department of Physical Geography, Faculty of Geosciences, Utrecht University, Utrecht, The Netherlands

Key Points:

- Sea-level rise increases dredging volumes in estuaries and the additional sediment delivered by sea-level rise quickly infills deepened channels
- Dredging creates a new morphological equilibrium with channel positions becoming more fixed, but this equilibrium is disturbed by sea-level rise
- Many European estuaries are more likely to drown (loss of intertidal areas, risk to flood protection) due to dredging than sea-level rise

Supporting Information:

Supporting Information may be found in the online version of this article.

Correspondence to:

J. R. Cox,
j.r.cox@uu.nl

Citation:

Cox, J. R., Lingbeek, J., Weisscher, S. A. H., & Kleinhans, M. G. (2022). Effects of sea-level rise on dredging and dredged estuary morphology. *Journal of Geophysical Research: Earth Surface*, *127*, e2022JF006790. https://doi.org/10.1029/2022JF006790

Received 6 JUN 2022
Accepted 30 SEP 2022

Author Contributions:

Conceptualization: J. R. Cox, J. Lingbeek, S. A. H. Weisscher, M. G. Kleinhans
Formal analysis: J. R. Cox, J. Lingbeek
Funding acquisition: M. G. Kleinhans
Investigation: J. R. Cox, J. Lingbeek
Methodology: J. R. Cox, S. A. H. Weisscher, M. G. Kleinhans
Project Administration: M. G. Kleinhans
Software: S. A. H. Weisscher
Supervision: J. R. Cox, M. G. Kleinhans

Abstract Estuaries and deltas worldwide are facing land loss and drowning due to sea-level rise (SLR). Commonly home to ports, their channels are dredged and deepened for navigation. However, little is known about how such sediment management will interact with changing sediment transport patterns due to SLR. Using scale experiments, empirical relations and real world examples from global estuaries and deltas, we identify that dredging and SLR combined enhance bend migration whereas SLR alone leads to decentralizing of channels and drowning of intertidal area. In estuaries where channels are fixed, excess energy due to increasing tidal prism will manifest as bed and bank erosion, placing flood safety measures like dikes at risk. SLR increases dredging volumes in upstream reaches due to the rapid collapse of shoals and river banks along the whole estuary. Channel deepenings are ineffective under SLR conditions due to sediment import induced by increasingly flood-dominant tides. Non-dredged systems which have more regular and level elevations will lose intertidal area more quickly than dredged systems that have disconnected higher intertidal flats and a single deep channel. Mid-size dredged European systems are more likely to drown due to dredging in the present century than from SLR. Effects can be avoided by pursuing sediment management strategies that help restore the morphology disrupted by dredging.

Plain Language Summary River channels are often dredged to allow access for large ships to seaports. Sea-level rise (SLR) will put coastal areas under pressure, as river channels deal with higher water levels and flood safety concerns, but arguably SLR could also lead to less intensive dredging efforts. We study the effect of SLR on natural versus dredged channels using scale experiments of river mouths to determine how SLR will affect dredging practice and the effects it will have on the channels (will they erode?) and surrounding areas (will they drown?). We have found that dredged channels show more erosion and bank collapse than non-dredged systems. Dredging volumes will also increase due to SLR so that dredging will have to take place more frequently and will cost more in the future. Many European estuaries are presently more likely to drown due to the effects of dredging than because of SLR. These adverse effects can partly be mitigated by sediment management that accounts for the natural sand transport processes and shapes of channels and bars.

1. Introduction

Estuaries are bodies of water with one or more open connections to the sea (Leuven et al., 2016) which develop at the land-sea interface due to delivery of sediment from both rivers and the coast (Nicholls et al., 2020). Estuaries that have developed naturally tend to have a converging planform shape, often with mutually evasive ebb and flood channels which create a multi-channel system (Jeuken & Wang, 2010; van Dijk et al., 2021; Weisscher et al., 2022). They have several intertidal shoals and bars, particularly at their widest points (Leuven et al., 2016), and extensive floodplains (van Veen et al., 2005).

However, many estuaries globally are now changing to a new enforced equilibrium as they are increasingly altered by human activities. The plains surrounding estuaries and deltas are rapidly urbanizing, leading to a variety of economic, environmental and ecological questions and concerns regarding long-term sustainability and management of these human-influenced systems (Loucks, 2019). Width is dramatically reduced as floodplains are embanked and intertidal areas are reclaimed, to be used for housing, ports, harbors and development of urban centers (Cox et al., 2022). Meanwhile, flood protection structures such as dikes, groynes and flood barriers are often implemented, redirecting flow and altering sediment transport regimes (O'Dell et al., 2021; Ten Brinke et al., 2004). Estuary depth is also commonly increased by dredging at a variety of scales.

Estuaries are commonly identified as hotspots for climate risk (Hill et al., 2020) because they are uniquely threatened by both sea-level rise (SLR) and river basin-wide climate changes (e.g., glacial melt, temperature

Validation: J. R. Cox, J. Lingbeek, S. A. H. Weisscher
Visualization: J. R. Cox, S. A. H. Weisscher
Writing – original draft: J. R. Cox
Writing – review & editing: S. A. H. Weisscher, M. G. Kleinhans

variation, changes to discharge) (Wong et al., 2014). They are also under pressure from dredging and sand mining (Bendixen et al., 2019; Cox, Dunn, et al., 2021) undertaken to create deeper shipping fairways for navigation, which has the added effect of removing the necessary sediment to maintain elevation and build/perpetuate estuary morphology. It is still unclear how the morphology and hydrodynamics of such dredged systems will respond to SLR and how this response will differ compared to natural, undredged estuaries. Moreover, how SLR will affect dredging volumes and dredging locations in estuaries is currently poorly understood. Whether adverse effects of SLR are exacerbated by dredging remains, therefore, unknown.

Dredging activities can be broadly split into two categories: (a) capital dredging events, which deepen channels permanently, and (b) maintenance dredging, which is the periodic process of keeping channels at a specific depth. Typically, systems undergo capital dredging every 10–20 years, while maintenance dredging typically occurs year-round, particularly in systems that are home to large ports (Cox, Dunn, et al., 2021; Cox, Huismans, et al., 2021; van Dijk et al., 2021). The dredged material can be either completely removed from the system (sold to market or dumped offshore) or reused and relocated within the system. Choosing locations for dumping this dredged material is usually based on two factors: keeping transport costs low, and whether natural sediment circulation within the tidal system can be used (van Dijk et al., 2021). To keep costs low, the material tends to be relocated as close to the dredging site as possible. Relocation in specific areas for example, intertidal shoals ensures re-circulation of this sediment within the estuary over time and can be used to protect or retain morphology (Maes et al., 2005; Monge-Ganuzas et al., 2013; van Dijk et al., 2019).

Dredging is becoming more common in estuaries globally and disrupts hydrodynamics (Nichols, 2018; Vellinga et al., 2014), sediment transport (Cox, Huismans, et al., 2021; van Maren et al., 2015), morphology (Jeuken & Wang, 2010) and ecosystems (De Vriend et al., 2011). An overview of the consequences of dredging and dumping activities on estuary hydrology and morphology can be found in van Dijk et al. (2021). To summarize: dredging causes tidal amplification (Temmerman et al., 2013); dredging causes increased flood dominance of tidal asymmetry (van Maren et al., 2015); dredging smooths channels, removing obstructions, changing the flow velocity and sediment transport profiles of the channels (Nichols, 2018); dredging and dumping creates deep channels and high intertidal areas, creating a disconnected single channel system (wherein flow paths and sediment connectivity are disrupted).

To date, several modeling and empirical research studies have been undertaken on the effects of SLR on estuaries. However, many of these studies are limited to the response of individual salt marshes (Kirwan et al., 2016) or individual systems (Hong et al., 2020; Hong & Shen, 2012; Vellinga et al., 2014; White et al., 2019). The effects of dredging are also not explicitly incorporated in these studies. Nonetheless, they provide several hypotheses for how hydrodynamics of estuaries may change due to SLR. First, SLR increases the cross-sectional area of tidal channels by enlarging channel volume as a response to the change in tidal prism (Hijma & Cohen, 2011; Leuven et al., 2019). How much and in what direction (vertically/deepening or laterally/widening) channel volume will be altered is dependent on several factors, primarily: the presence or absence of lateral/vertical constraints on channels, including bank stability and overflow depth (Kleinhans et al., 2022), and how much SLR decreases channel bed friction and resulting changes to flow velocity (Wachler et al., 2020). A further important interaction is the potential effect of SLR on flood storage (as a result of a loss of intertidal bars and shoals), which changes the tidal prism of the system and can in turn cause growing or shrinkage of the estuary.

As SLR increases the tidal prism, it promotes the expansion of channel cross-sections (Stefanon et al., 2012), and alters tidal prism-area relations for tidal channels. If the width is constrained or the banks protected, and sediment supply is limited, bars may be subdued and channels may become shallower (Leuven et al., 2019). In estuaries with unrestricted tidal entrances (wide estuary mouths), SLR can cause tidal waves to propagate further inland increasing tidal effects upstream (Khojasteh et al., 2020). It has also been suggested that SLR can restore intertidal areas by reconnecting deep dredged channels with surrounding plains (van Dijk et al., 2021).

However, disentangling the effects of dredging and SLR is difficult because both processes change sediment transport patterns and morphology. SLR, through modifying tidally averaged depth, may display similar effects on hydrodynamics as those of dredging, that is, increasing tidal propagation and modifying tidally averaged depth (Cai et al., 2012).

Here, we hypothesize that the changes in hydrodynamics caused by SLR also cause significant changes to bank erosion and tidal meandering. In the absence of bank protection, channels naturally meander over time as outer bends erode and sediment is deposited on the inner bend. Meandering is determined by feedbacks between channel morphodynamics, channel migration, channel erosion, and evolution, which are driven by the interactions between water and sediment (Kleinhans, 2010). In the fluvial-tidal transition zone, there are many large meanders with tight bends. These meanders tend to become larger in a seaward direction and the dimensions of these meanders are proportional to local channel width (Leuven, van Maanen et al., 2018). Meander amplitude is indicative of the maximum extent of erosion in the outer bend (Steijn et al., 2019).

We hypothesize that as SLR occurs, increased tidal prism will increase the overall channel volume and width of estuaries (Khojasteh et al., 2021; Leuven et al., 2019), thus increasing tidal amplitude of meanders, provided that mean sea-level is low enough to leave adjacent tidal flats undrowned. In tidal channels that have been dredged, tidal amplitude is increasing faster than in non-dredged channels (van Til, 2018). In systems that are freely meandering in their floodplains, the rate of migration is highly variable, with fast migration rates likely to be linked largely to a large sediment supply (Shimozono et al., 2019; Steijn et al., 2019). Comparing natural versus dredged systems, their meander migration rate can therefore be an important aspect of assessing erosion risks and future flood safety, but the effects on meander migration due to dredging in combination with SLR remain unclear.

Using scale experiments, we can test both hydrodynamic and morphological effects and isolate the processes of SLR, dredging and their interaction. Here, for the first time in an experimental setup, we quantify the influence SLR has on estuarine morphology in dredged versus undredged estuaries. We focus on location and migration of channels, bank instability, sinuosity, and intertidal area development. We also identify how SLR influences dredging locations and volumes. We then relate these observations to global systems, current patterns and future predictions and current estuary and delta management and policy surrounding SLR and dredging.

2. Materials and Methods

Scale experiments have proven useful in identifying and confirming empirical estuary processes and relations, including the identification of channel and bar patterns (Leuven, Braat, et al., 2018), the influence of mud (Braat et al., 2019) and of vegetation (Kleinhans et al., 2022) on morphological development, the influence of dredging on multi-channel tidal systems (van Dijk et al., 2021) and the long term development of infilling estuaries (Weisscher et al., 2022). These experiments have been proven to be robust in recreating meaningful and accurate estuarine hydrodynamics (Weisscher et al., 2020) and morphodynamics (Leuven, Braat, et al., 2018) at a small scale and will therefore be used to assess the effects of SLR on dredged and non-dredged alluvial estuaries.

This research builds on two previous estuary experiments of (a) a control experiment of an alluvial sandy estuary (Leuven, Braat, et al., 2018) and (b) a dredged estuary with otherwise the same conditions (hereafter: "+DR") (van Dijk et al., 2021). To isolate the effects of SLR and dredging, two novel experiments were conducted: (c) an alluvial sandy estuary with SLR (hereafter: "+SLR") and (d) a dredged estuary with SLR (hereafter "+DR +SLR"). In total, four experiments were analyzed and compared. Below, the experimental setup and procedure is given in more detail, followed by the steps undertaken for data analyses.

2.1. Experimental Setup and Procedure

The Metronome is a tilting tidal flume, which is designed to specifically replicate alluvial estuary systems, particularly like those on the Dutch coast. A full overview of how the Metronome is designed and how it functions can be found in Kleinhans et al. (2017). The 20 m by 3 m flume combines a river feeder, a wave generator and tidal effects (accomplished by the tilting of the flume—see Figure 1) to simulate estuarine hydrodynamics and morphological development.

All four experiments had the same initial settings and a baseline of hydrodynamic boundary conditions. A 7 cm thick sand bed was placed in the flume, which was 18 m in length (from 18 to 20 m is an imposed sea—see Figure 1) with an idealized 3 cm deep channel which exponentially widened in the seaward direction (see Braat et al., 2019; Leuven, Braat, et al., 2018). The banks of the initially carved channel are freely erodible and all sediment is conserved within the flume. Sediment input in these experiments comes from the adjacent floodplains and reversing flow (Kleinhans et al., 2017) whilst in reality, sediment input comes from both upstream (fluvial boundary) and downstream (coastal boundary). The effect of this difference is examined in the Discussion.

Journal of Geophysical Research: Earth Surface

10.1029/2022JF006790

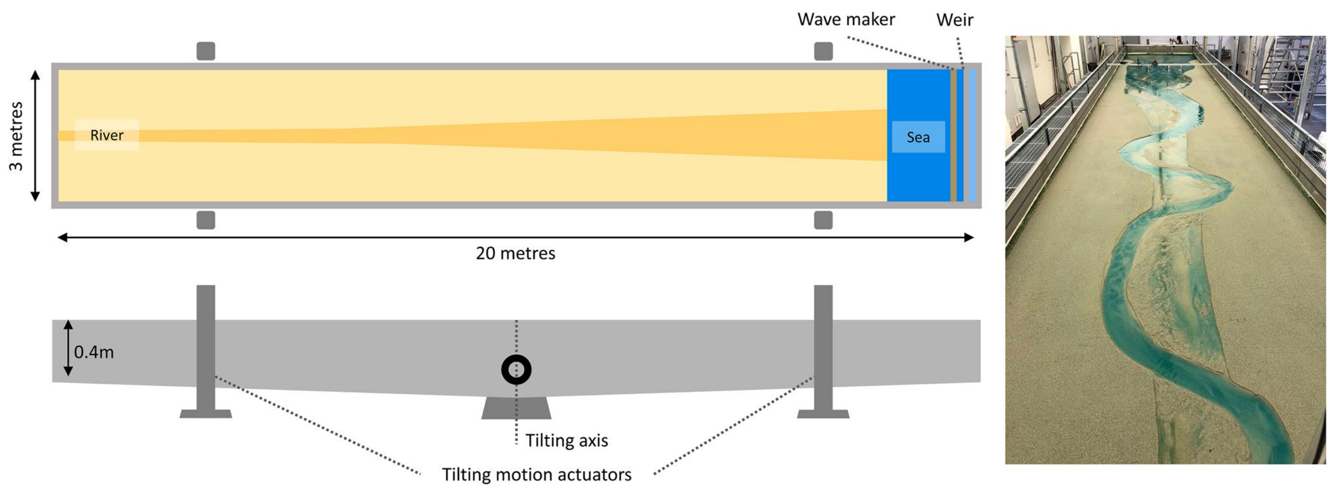

Figure 1. Sketch of the experimental setup indicating river and sea boundaries and the tilting function which simulates tidal action and a photograph of the experiments.

The flume tilted with a period of 40 s at a slope amplitude of 7.5×10^{-3} m/m to generate ebb and flood tidal flows. The initial water level was set to 65 mm at the seaward boundary, leading to a mean water level of 25 mm above the channel floor and of 5 mm below the erodible floodplain elevation. Water level in the flume is controlled by adjusting a weir at the seaward boundary. River discharge entered the estuary at the upstream boundary at a rate of 100 L/hr during the ebb phase only. No sediment was added to the river discharge. Waves were generated by a horizontal paddle at the downstream boundary with a frequency of 2 Hz and an amplitude of 3 mm during the flood phase only. These baseline initial and boundary conditions were based on the work of Leuven, Braat, et al. (2018) and van Dijk et al. (2021), and morphology was allowed to develop for 3,000 tidal cycles in all four experiments before any interventions were undertaken. These interventions of dredging and SLR followed the protocols that are outlined below.

2.1.1. Dredging Protocol

Dredging in most estuaries can be divided into two types: capital dredging or channel deepening events and maintenance dredging. Capital dredging events are once-off events, which aim to permanently deepen channels. Maintenance dredging is the regular activity of dredging to maintain channels to their required depth. Both types of dredging were simulated in the experiments. Dumping is the placement of dredged material in different locations in the estuary. In these experiments, we followed the dredging and dumping protocol of the closest equivalent estuary type (sandy, dredged estuary), that is, the Western Scheldt, the Netherlands, and scaled all width and depth changes due to dredging, frequency of activities and dredging and dumping strategies based on its protocols (see van Dijk et al., 2021, for more information). The same dredging and dumping protocol was applied to the experiments +DR and +DR + SLR.

Morphology was first created in the first 3,000 tidal cycles, after which an initial capital dredging event took place to create a dredged channel of 3 cm depth at 3,000 tidal cycles (20% depth increase; past channel deepenings in the Western Scheldt range from ∼20% to 25%). The dredged channel was also widened to a scaled width relative to the total width of the estuary (see van Dijk et al., 2021, for more information) and this width remained fixed for the course of the experiments. Dredging was undertaken by hand using a palette knife. This newly dredged channel was then maintained and dredged periodically five times, every ∼50 cycles. A second capital dredging was then undertaken to deepen the channel to 3.5 cm (4,600 cycles). This new channel was dredged five times, every ∼100 cycles. After this, dredging was ceased and morphology was allowed to further develop until the end of the experiment, from 5,100 tidal cycles onward to 11,000 cycles.

Material dredged in the capital dredging events was completely removed from the system as is standard for capital dredging events (see van Dijk et al., 2021, for more information). However, material removed during maintenance dredging events was dumped back into the system. All dredging volumes were measured. The equivalent amount of dry sand was placed in the nearest suitable dumping location to where the material was removed (pits, shoal

10.1029/2022JF006790

Table 1
Comparison of SLR Rate in the Experiments Relative to Predicted Change in Water Depth in the Main Navigation Channel Due To SLR of Estuaries and Deltas Globally

Delta/estuary	Timespan	Additional water in navigational channel at the mouth due to SLR (%)	Source
Non-dredged experiment	Each SLR event	8%	Leuven, Braat et al. (2018)
Dredged experiment	Each SLR event	5%–7%	van Dijk et al. (2021)
Rhine-Meuse	80 years	7%–12%	KNMI (2021)
Western Scheldt	80 years	8%–13%	KNMI (2021)
Mekong	35 years	1.3%	Dunn and Minderhoud (2022)
Pearl (Zhujiang)	80 years	7%–20%	Hong et al. (2020)
Yangtze	80 years	8%–13%	Chen et al. (2016); Zhang et al. (2019)

edges, side channels). Sediment designated (due to proximity) for dumping on shoals is placed on shoal edges to encourage overwash of sediment onto the entire shoal.

2.1.2. Sea-Level Rise Protocol

A variety of SLR conditions were tested in pilot experiments to determine the most appropriate scaling for the experiments. Our SLR condition estimates were based on Intergovernmental Panel on Climate Change (IPCC) AR6 (2021) projections for global sea-level rise (Masson-Delmotte et al., 2021) and Royal Netherlands Meteorological Institute (KNMI) predictions for the Western Scheldt for 2021 (KNMI, 2021). To translate these rates for our scaled experiments, we calculated the total SLR as a fraction of the water depth in the deepest channel at the estuary mouth (Table 1). These tests indicated that the water level should rise 2 mm per 1,000 cycles which was an increase of ~8% water level in the non-dredged channels and ~5%–7% in the dredged channels (Table 1). SLR was induced four times during the experiments to have a total of 8 mm of SLR (4 steps of 2 mm). At cycle 6,000 SLR was ceased to observe the long term development of morphology after SLR.

2.2. Data Analysis

To perform analysis on morphology, digital elevation models (DEMs) were created. DEM capture required a completely dry bed, thus water was gradually drained from the flume, ensuring no morphodynamic perturbation took place. Observations of the flume during the experiment indicated that indeed no significant morphodynamic changes occurred during drainage (only minor cuts in the ebb delta or sills which disappeared within 1–2 cycles of restarting the flume). Consecutive oblique pictures were taken of the dry bed using a digital single-lens reflex camera. The images were then processed using the structure-for-motion software Agisoft Metashape Professional, version 1.6.4. DEMs were acquired every ~1,000 cycles for the non-dredged experiments for 11,000 cycles in total. For the dredged experiments, this procedure was extended, with extra DEMs taken immediately before and immediately after each dredging event (capital or maintenance). DEMs were interpolated to a 14 × 14 mm grid size for geometric analyses and interpolated to a 50 × 50 mm grid size for tidal flow modeling, as explained further below.

The channel centerline was identified as the lowest path from river to mouth by an algorithm for channel detection (Sonke et al., 2022). The migration of meander bends and the overall change in river planform was quantified as sinuosity, which was computed as the length of the main channel divided by the valley length (i.e., 18 m). The hydrodynamics in the experiments were quantified using the two-dimensional numerical flow model Nays2D (Weisscher et al., 2020), in which shallow flows of at most a few centimeters can be accurately modeled. Nays2D takes as input a DEM and the corresponding boundary conditions to produce maps of water depth and flow velocity, for which bed elevation data were coarsened to a resolution of 2.5 by 2.5 cm to limit computational time. The flow modeling was done for all experiments at 3,000, 5,000 and 11,000 cycles including effect of SLR and used to quantify the development of intertidal areas and along-channel tidal prism.

The tidal prism (P) and cross-sectional area (A_r) of channels have a near-linear relation, derived from empirical data in natural tidal systems (e.g., Jarrett, 1976; Leuven, De Haas et al., 2018; O'Brien, 1931, 1969). This means that the tidal prism–cross-sectional area relationship may indicate if channels are close to their equilibrium bed level. For example, this relationship stipulates that a tidal channel too shallow for its tidal prism will tend to erode, whilst channels too deep for their tidal prism will tend to accrete. The classic relationship is given as $A_r = kP^{\alpha}$, where k and α are constants (see Leuven, De Haas et al., 2018, for review on parameter values). However, these constants k and α ignore friction effects that are much larger for tidal scale experiments, which makes a fair comparison between real-world systems and scale experiments difficult (Kleinhans et al., 2015; Mayor-Mora, 1977; Seabergh et al., 2001; Stefanon et al., 2010). The formulation by O'Brien (1969) accounts for these friction effects, assuming flood and ebb duration and peak ebb and flood velocities are similar:

$$A_r = cP^{\alpha} \quad \text{with} \quad c = \pi (TU_{\max})^{-1} \tag{1}$$

where T is the tidal period (s), $U_{\max}$ is the peak cross-sectionally averaged flow velocity during flood or ebb (m/s), and $\alpha = 1$. Consequently, this revised Equation 1 collapses scale experiments and real-world systems on a single line, enabling a fair comparison between the two (e.g., Seabergh et al., 2001). In the experiments, cross-sectional area was computed for mean sea-level, including the effects of SLR. The tidal prism was determined as half the sum of absolute tidal discharge over a tidal cycle.

To assess the migration of meander bends and the overall change in river planform, sinuosity changes over time were assessed using Equation 2 following from (Rust, 1977).

$$S = \frac{L_{arc}}{L_{abs}} \tag{2}$$

where S is channel sinuosity, L_{arc} is the length of the channel along the centerline, and L_{abs} is the straight line distance from the start to end of the channel. Both L_{arc} and L_{abs} were determined for the "main" river channel (see *Dredging Protocol*) using the DEMs of each experiment in ArcGIS.

Finally, the experiments were compared to real-world systems in terms of expected sediment budgets and land loss under different climate scenarios. The present sediment budgets for global deltas were derived from the delta database of Nienhuis and van de Wal (2021). The sediment budget was calculated as the sediment flux from rivers minus the accommodation created by SLR. These sediment budgets were then combined with reported maintenance dredging values for various systems (Anthony et al., 2019; Arnaud-Fassetta, 2003; Cox, Huismans, et al., 2021; Frey & Coe, 2020; Frihy et al., 2015; Habersack et al., 2016; Jordan et al., 2019; Kemp et al., 2014; Liu & Zhang, 2019; Marineau & Wright, 2015; Rudra, 2014; Smets et al., 1997; van Dijk et al., 2021; van Maren et al., 2015; Weilbeer, 2014; Wu et al., 2018) (see Data Set S1 for full overview).

3. Results

This section outlines the main findings from the experiments. In the Discussion, limitations of these experiments and validity of results is explored and connected with global estuaries and deltas.

3.1. Estuary Development

In general, all the experiments exhibited three morphological zones: (a) upstream river with shore-connected bars (0–6 m), (b) multi-channel middle estuary with bars and shoals (6–16 m) and (c) wide downstream seaward section and delta (16–20 m). In the non-dredged experiments, the upstream river area is gently meandering and narrow, transitioning to a wider multi-channel system in the middle and seaward sections, where bars and channels change over the course of the experiments (see differences between 5000 and 11,000 cycles in Figure 2). The influence of sea-level rise in the non-dredged experiments is most marked in the seaward part of the system and the delta. Sea-level rise causes a much wider estuary downstream as banks are attacked more frequently and with higher flow velocities. The delta in the SLR only case becomes much higher in elevation because of a marked change in along-flume sediment redistribution. There is enhanced deposition on the delta top and lower reaches where sediment is plentiful, but erosion in the upper reaches due to a lack of available sediment as the lateral sediment transport profile is altered, in the sea-level rise case. In the middle and upstream part of the system, shoals are smaller and fewer in number due to sea-level rise and the intertidal area is significantly decreased.

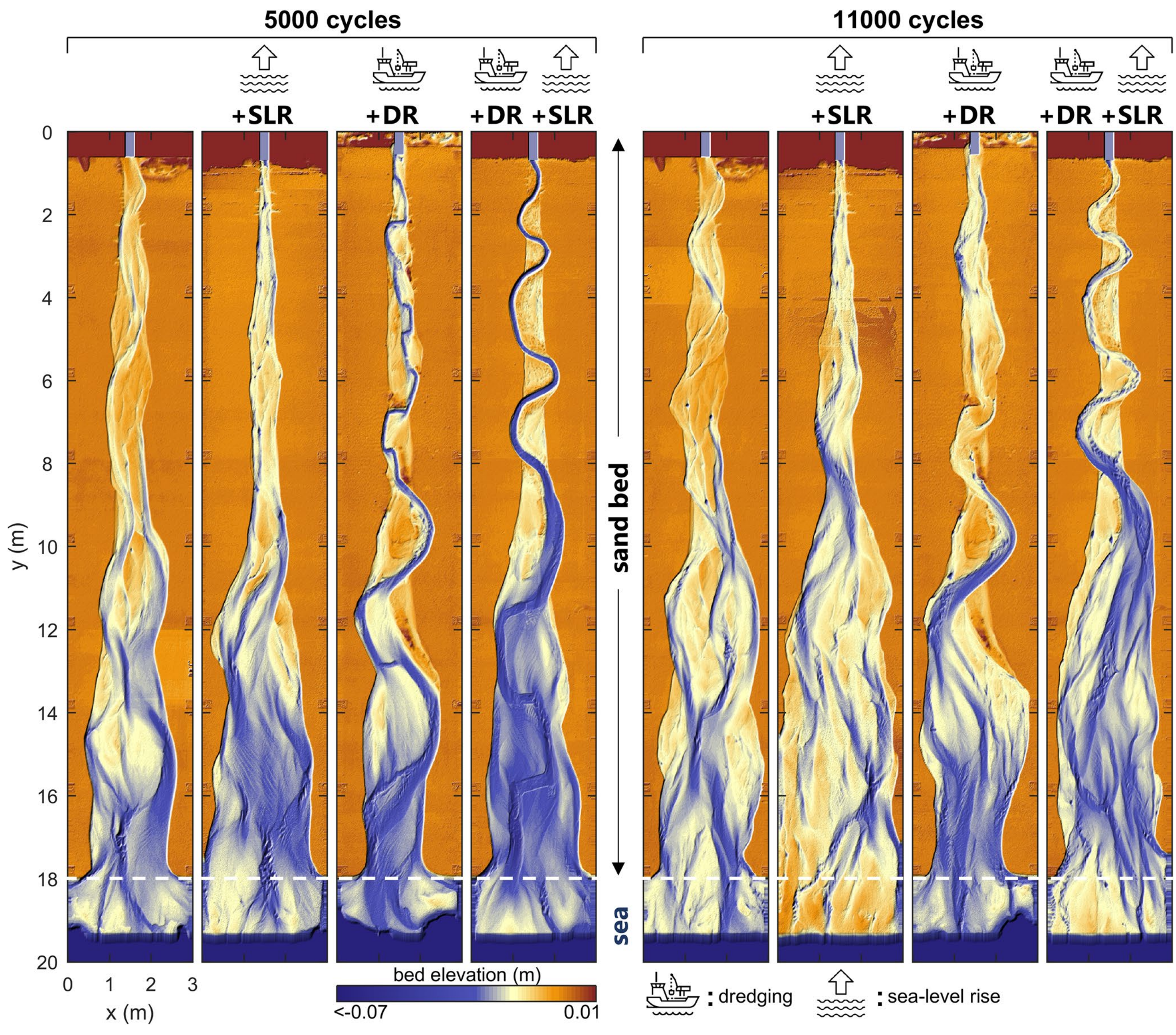

Figure 2. Digital elevation model of all four experiments at cycle 5000 (mid-experiment, after which point no further dredging was done) and at cycle 11,000 (final morphology). Icons refer to experiments with DR = dredging and SLR = sea-level rise.

In both dredged experiments, the dredged channel can be clearly seen during the experiments but it also persists long after dredging has stopped. SLR leads to even further long-term persistence of the dredged channel. The new fixed channel is surrounded by high shoals and bank-attached bars in the upstream and middle sections. The delta area is significantly smaller in the dredged experiments. Shoals in the dredged experiments are larger and become fixed in place due to repeated disposal of dredged material (see Material and Methods and (van Dijk et al., 2021) for more information).

SLR causes a much wider seaward estuary section and higher delta. Meanwhile, the large shoals that formed and stabilized in the middle stages of the experiment (3000–6000 cycles) without SLR (at 10–12 m and 14–16 m, see panels 1 & 3 of Figure 2) are no longer formed or fixed under SLR conditions. Instead, the location of fixed shoals shifts upstream (to 4–6 m and 8–10 m) in the estuary. SLR in combination with dredging also causes intense meandering in the upstream part of the system as the large meander bends that typically formed in the middle part of the estuary, migrate upstream due to SLR. The bends expand rapidly as the outer banks are attacked with increasing flow velocities.

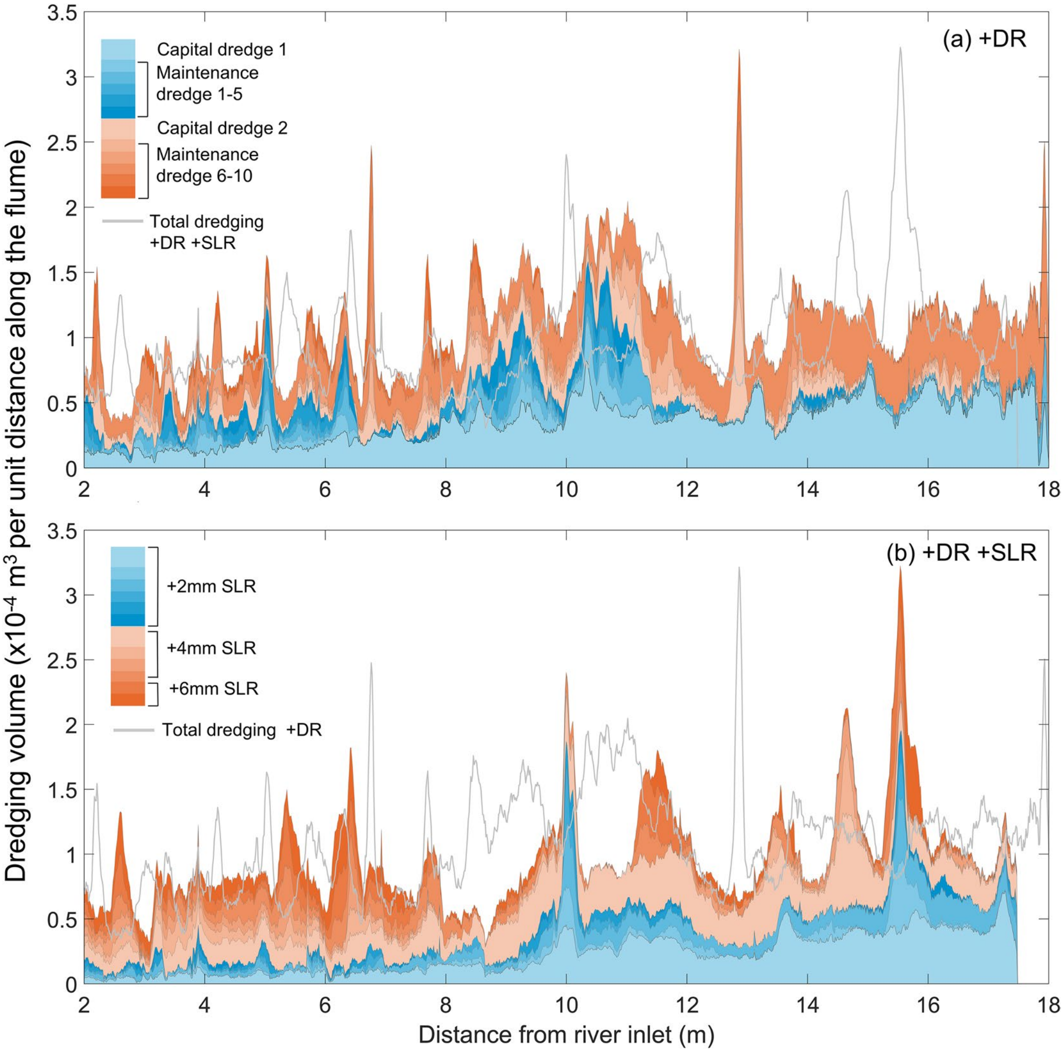

Figure 3. Total dredging volume per unit distance along the flume for (a) the dredged experiment without SLR, where the gray line represents the total dredging volume per cell size for the dredged experiment with SLR and (b) the dredged experiment with SLR, where the gray line represents the total dredging volume for the dredged experiment without SLR. Unit distance is 14 mm (DEMs were interpolated to a cell size of 14 × 14 mm). The equivalent volume of dredged volume was dumped back into the system as per the dumping protocol outlined in the Methods.

3.2. Dredging Volumes and Locations

SLR not only changes the overall volumes of dredging, but it also changes the most prominent dredging locations along the estuary (Figure 3). In the no SLR experiment, the initial capital dredging is higher than in the SLR experiment. This is due to variation in initial shape of the estuary and relative dimensions of existing channels pre-dredging. Both experiments show similar overall volumes of dredging for the first cycle of maintenance dredging (events 1–5). However, there is a clear and marked difference in the total amount of sediment dredged during the second capital dredge (which coincides with the second SLR increase), with SLR requiring more volume to be dredged during a capital dredging event. Consequent maintenance dredging volumes (events 6–10) were also in total consistently higher due to SLR. In the Western Scheldt estuary, volumes of capital dredging are typically ~0.005% of the total estuary area while maintenance dredging volumes are ~0.003%. In the non-SLR experiment and SLR experiments, capital dredging volumes were averagely ~0.03% and ~0.03% of the total estuary area while maintenance dredging events were averagely ~0.008%, and ~0.01% respectively. A comparison of these dredging volumes relative to several other global systems is presented in the Discussion.

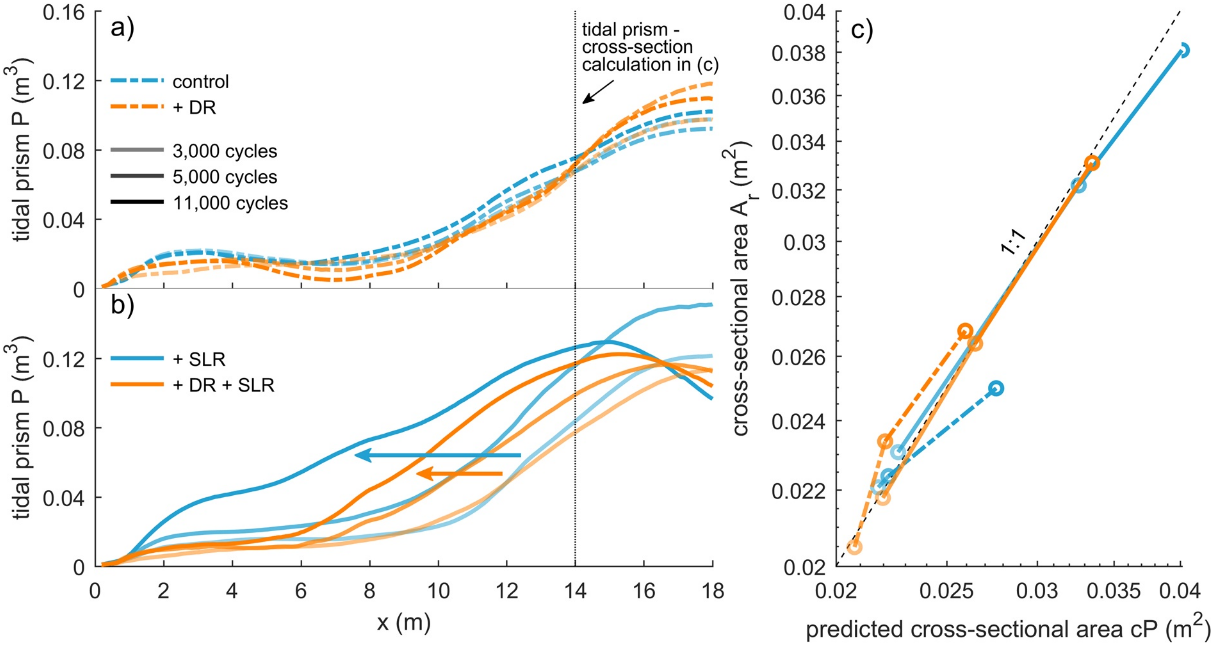

Figure 4. (a) Development of the tidal prism along the estuary for the experiments with and without dredging with a constant sea-level and (b) with sea-level rise at 3,000, 5,000, and 11,000 tidal cycles. (c) Measured cross-sectional area versus predicted cross-sectional area cP (i.e., tidal prism P multiplied with a friction-dependent coefficient c, following Equation 1), with tidal prism increasing in the experiments over time. The color intensity of lines represents the timestep (cycle number), where light orange/blue = 3000 cycles, medium orange/blue = 5000 cycles, and dark orange/blue = 11,000 cycles.

The dredging locations are also markedly different. SLR meant that dredging was more consistently required everywhere in the system. Without SLR, specific target areas required consistent and high volumes of dredging that is, where sills built up, or locations where ebb and flood channels were unnaturally connected due to dredging. Some clear peaks can be identified in both experiments. In Figure 3a, peaks can be identified at ~6.5 m and ~13 m. These locations are both areas where ebb and flood channels were manually linked to create one smooth flood channel ("crosses") and are typically areas where sills build up. Meanwhile, looking at Figure 3b, the major peaks occur at ~10 m and ~15.5 m. The first peak corresponds to a location which cut through a bar/shoal and experienced continuous bank collapse and infilling as a result. The second was another so-called cross, which as SLR continued to increase, did not require as much dredging.

In general, higher volumes of dredged material needed to be consistently removed farther upstream in the latter stages of the +DR + SLR experiment (compare orange/red areas of ~4–8 m in Figures 3a and 3b). Whilst in the +DR experiment, most material was removed downstream of 10 m in the second set of maintenance dredges. This suggests that maintenance dredging locations are moving upstream with SLR.

3.3. Response of Channels—PA Relations

In general, our dredged estuaries show a smaller tidal prism than non-dredged systems (Figure 4a). They have a typically smaller cross-sectional area and thus a smaller tidal prism. In the dredging only experiment (+DR) the tidal prism increases in the downstream part of the system (delta area). The accumulation of sediment in the middle of the flume after dredging has ceased also causes a decrease in cross-sectional area upstream of this location (2–10 m).

SLR significantly alters the tidal prism. The tidal prism not only increases its total volume but also, the tidal prism increases in a landward direction. This effect is most prominent in the non-dredged sea-level rise experiment (+SLR). SLR causes a gradual but overall large increase in tidal prism in all locations in the estuary. The tidal prism increases gradually in the upstream reaches over time (see arrows in Figure 4b). In the experiment with dredging and SLR (+DR + SLR), the total tidal prism increase is less, and the increase in the upstream reaches is slower. Tidal prism is also slightly decreased as flood storage is decreased. Flood storage areas are lost as intertidal areas become drowned under SLR. This effect is most significant in the final stages of the non-dredged

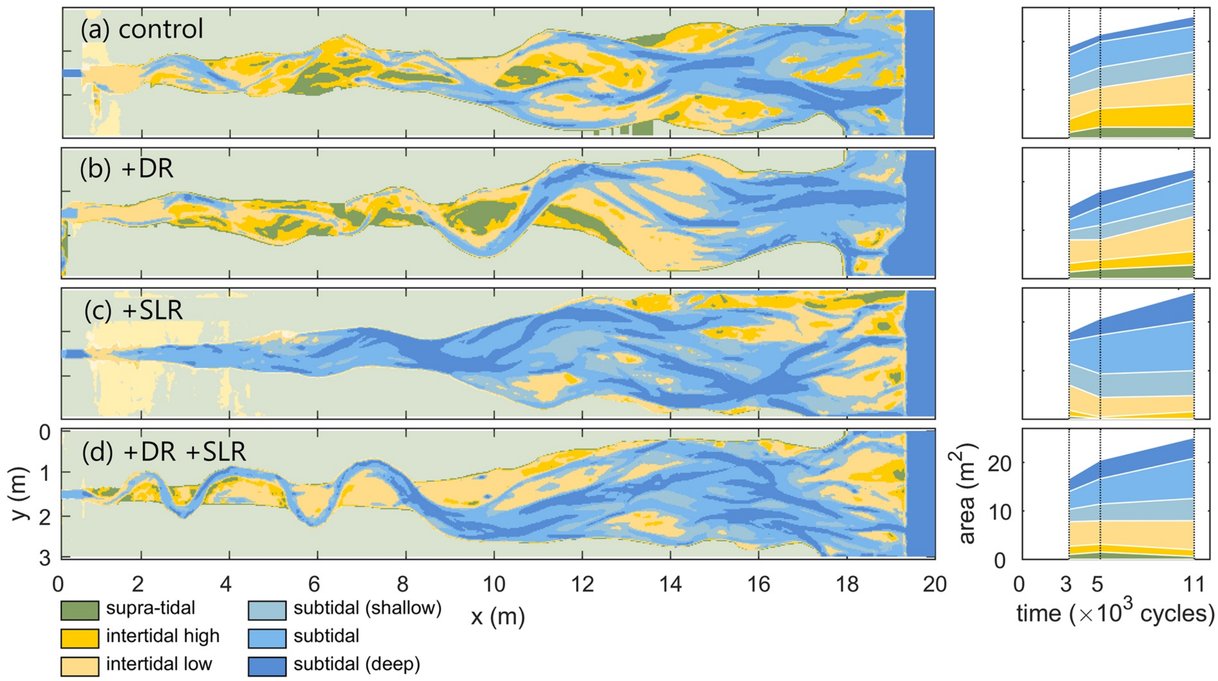

Figure 5. Maps of the subtidal, intertidal, and supratidal area at cycle 11,000, and the temporal development of the surface area of these areas for the active parts of the estuary, disregarding the unreworked (transparent) floodplains, for (a) the control experiment with no dredging and no SLR, (b) the dredged experiment with no SLR, (c) the SLR only experiment and (d) the dredging and SLR experiment, where tidal range at the entrance is 0.0015 m, 0.0022 m, 0.0034 m, and 0.0030 m, for experiments a, b, c, and d, respectively.

experiment where most of these flood storage areas have drowned (see Figure 4b—the darkest blue line (cycle 11,000) is below the medium blue line (cycle 5,000)).

The dredged-only (+DR) experiment tends to have a slightly higher cross-sectional area than predicted (Figure 4c). In contrast, the control experiment without dredging or sea-level rise has a lower cross-sectional area at the end of the experiment than predicted. These discrepancies are most likely caused by the prediction cP, which assumes a perfectly sinusoidal tidal wave with equally large peak ebb and flood currents. However, in response to dredging and natural development, a bathymetry developed with multiple channels and bars that slightly deform the imposed tidal wave, which results in the slight deviations from the predicted cross-sectional area. Besides such small deviations, the relation between cross-sectional area and tidal prism generally also holds for the flume experiments.

3.4. Intertidal Area

In the absence of SLR and dredging, the experiments tend to develop relatively even proportions of subtidal area to intertidal and supratidal area. By the end of the experiment (Figure 5a), there is a high amount of inter- and supratidal area in the upper and middle parts of the flume. SLR radically changes this pattern. In the absence of dredging, SLR decreases the intertidal area and increases the subtidal area, and the supratidal area is nearly entirely eliminated (Figure 5c). In particular, the upper and middle parts of the flume lose all their intertidal area. There is also significant overbank flooding in the upper part of the flume due to excess water.

Dredging alone tends to decrease the overall estuary area. The proportion of subtidal to inter- and supratidal area remains even. The upper and middle parts of the system have high proportions of intertidal area but several sections are also cut off from tidal influence, particularly as the dredged channel infills in the absence of dredging.

Dredged systems actually retain more of their intertidal area than non-dredged systems under SLR (Figure 5d). SLR also increase the total estuary area. The intertidal areas in the upper and middle parts of the system persist, and SLR decreases the amount of supratidal areas, reconnecting the main channel with intertidal areas and floodplains. However, significant intertidal area in the seaward part of the system is lost.

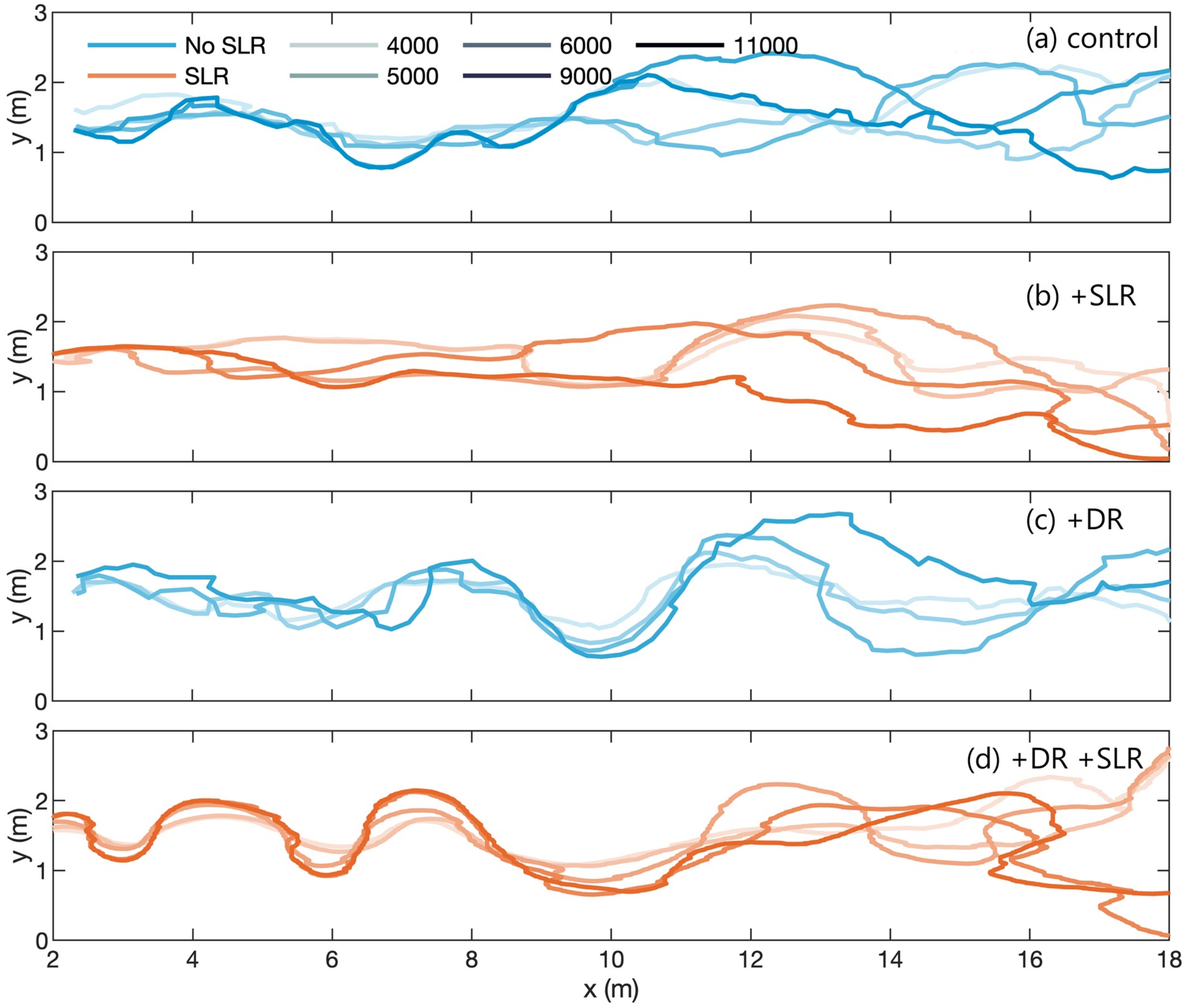

Figure 6. Location of the main channel for (a) the control experiment, (b) the non-dredged, SLR experiment (c) the dredged, no SLR experiment and (d) the dredged, SLR experiment.

3.5. Channels, Migration, and Sinuosity

Figure 6 shows the location of the main channel during all four experiments. There is clear differentiation between the non-dredged (Figures 6a and 6b) and dredged (Figures 6c and 6d) channels. In the non-dredged cases, the channel is free to migrate and does so extensively during the experiments as flow switches between ebb and flood channels. When SLR is added, in the undredged conditions, migration rates are higher, particularly in the upstream and middle sections of the estuary. In the case of the dredged experiments, SLR leads to the erosion of the fixed channel in the middle and upstream reaches. In the downstream part of the system, there is increased and unpredictable channel switching and high migration rates.

4. Discussion

The following section outlines the limitations of the experiment and compares the results of the experiments with our predicted outcomes (as per the introduction). It then considers the effect of SLR, dredging and the combination of both processes on estuary morphology and finally culminates with the implications of our findings for estuary management.

4.1. Limitations of the Experiment and Comparison With Real Estuaries

There are some key factors absent from the experimental setup that are present in real-world dredged urban systems. These include (a) lateral restrictions that is, embankments, dikes, (b) vertical restrictions that is, subsurface geology or hard clay layers and (c) flood and discharge control structures that is, dams, sluices.

Nearly all major urban deltas are diked and embanked (O'Dell et al., 2021). Their river courses have been fixed for tens or hundreds of years (Cox et al., 2022) and are no longer free to laterally expand and migrate. However, the experiments require lateral expansion to accurately recreate sediment transport (see (Braat et al., 2019; Kleinhans et al., 2017; Leuven, Braat, et al., 2018)). Similarly, many estuaries have hard clay layers present in their subsurface which can determine channel depths and shapes (Pierik et al., 2022). They can halt erosion of channel beds and affect natural tidal-prism area relations (Cox, Huismans, et al., 2021). Many of these hard layers will be present as systems move upland due to SLR, acting as an important control on depth in the future (Pierik et al., 2022).

The experiments represent idealized estuaries with uninterrupted flow and sediment transport connectivity (Sonke et al., 2022), but many urban systems have upstream dams and downstream sluices which determine the flow of both sediment and water (Cox, Huismans, et al., 2021; Nienhuis & van de Wal, 2021; van Wesenbeeck et al., 2014). These structures can divide and separate the effects of SLR unevenly in different parts of the system. Furthermore, river discharge is constant during the experiment, as are tides. In reality, high discharge events, storm surge events and variations in the seasonal hydrodynamic climate can cause extreme episodic events which are important in terms of morphological development and response (Cox, Dunn, et al., 2021; van den Hurk et al., 2014; van der Deijl et al., 2017). These could not be accurately recreated in our experimental facility with any degree of confidence.

As outlined in the Methods, the sediment used to build estuary morphology in our experiments comes from erosion from the adjacent floodplains by the ebb and the flood flow (Kleinhans et al., 2017). Therefore, when the tidal prism and volume of the experimental estuary is at a disequilibrium, the banks are eroded because the slope renders this sediment more mobile than that on the bed. The volume of sediment becoming available for intertidal bar formation and adjustment to imposed dredging and SLR is not limiting, as the banks were supratidal and can be eroded up to the flume sidewall. In real-world systems, it is usually a combination of fluvial sediment supply and sediment import from the coast which builds and shapes morphology, but the possibility of bank erosion is not excluded. The total availability and distribution of this sediment determines local morphological adjustments. This means local morphological response will be very case-study dependent, due to varied sediment delivery (see Data Set S1) which is also globally decreasing (Dunn et al., 2019) and varied effects on tidal prism (either an increase or decrease depending on estuary shape among other factors). However, in real estuaries, just as in our experiments, the disequilibrium of the tidal prism as caused by dredging and SLR causes large-scale morphological adjustment.

SLR in our experiments led to a marked along-flume alteration in sediment transport which led to a difference in internal redistribution of sediment compared to experiments without SLR, and most marked in the experiment +DR + SLR. This agrees with the work of Nichols (2018) who, on the basis of case studies and numerical modelling, hypothesises that dredging changes the sediment profile along channel by smoothing bathymetry. Our experiments extend this theory to include SLR: the estuary responds to the disequilibrium caused by dredging by adjusting its channel geometry through erosion and deposition; SLR enhances this disequilibrium and, depending on the rate of response to SLR, it can cause a marked difference in upstream and downstream morphological response, that is, quicker deposition of sediment in deep dredged parts of the system (downstream) and more extensive erosion in the upstream reaches.

In the SLR cases, the delta is higher in elevation than the non-SLR cases, as the accommodation space above the delta is filled. Our flume lacks littoral currents and unlimited accommodation space in the sea, which is in part the reason for these higher deltas. In reality, whether deltas lose, maintain or gain elevation in the face of SLR is dependent on the tendency to import sediment, the littoral dynamics and the available accommodation space (Ibáñez et al., 2014). We do not aim to accurately emulate delta development in this research, but it will have an important influence on tidal channel and inland river morphology, thus is a point for further investigation.

The dredging and disposal techniques were designed to be as realistic as possible. However, due to high dredging volumes and fewer available dumping locations than in the Western Scheldt, high volumes of sediment tended to end up on intertidal shoals. This elevated the supratidal areas at a faster rate than observed in case studies where dumping actually connects several smaller intertidal areas over time leading to a more gradual increase in elevation (van Dijk et al., 2021). In the +DR + SLR experiment, significant bank collapses of intertidal shoals and bars occurred producing sediment that had to be removed by dredging (these can be seen in Figure 2). Intertidal areas in reality will be slightly more stable due to the presence of mud and vegetation (Braat et al., 2017; Brückner et al., 2019; Kleinhans et al., 2022), but they will still frequently collapse in dredged systems (van Dijk et al., 2019).

Many estuaries are also experiencing enhanced stratification due to dredging, causing an estuary turbidity maximum as suspended sediment is rapidly trapped, sometimes causing hyperturbid estuaries (Burchard et al., 2018; Talke & Jay, 2020; van Maren et al., 2015). Such marked stratification is technically impossible in our experiments as only freshwater is used, should be absent in our experiments with a maximum Canter-Cremers number of ~0.003 in all of the experiments, indicating a well mixed estuary. Here, the Canter-Cremers number is the ratio of freshwater to saline water where 1 represents a stratified estuary (see Savenije, 2005, for review on Canter-Cremers number). However, in stratified estuaries the interaction of salinity and density currents as sea-level rises may be an important factor in determining how much sediment will become trapped in estuary mouths (Hoitink et al., 2017; Niesten et al., 2021). Hyperturbidity and enhanced sediment trapping in turn determines sediment management in estuaries, as such enhanced sedimentation can increase dredging costs (Cox, Huismans, et al., 2021) or hinder navigation (van Maren et al., 2015), ultimately determining dredging locations and possibilities in the future.

4.2. Morphological Response of Estuaries to Dredging and SLR

Our experiments indicate that dredging volumes and total areas that need to be dredged will be increased in response to SLR. This larger spatial domain requiring dredging also seems to shift upstream due to SLR. Capital dredging events and channel deepening events essentially become ineffective due to SLR, particularly in the most seaward part of the system (downstream of 10 m, see Figure 3), due to fast sediment deposition induced by sea-level rise which returns the channel to the same depth as before the capital dredge. This seems in contrast to previous modeling of the Western Scheldt Estuary (van Dijk et al., 2021), which suggested a slight decrease in dredging volumes when SLR was imposed. A possible explanation is that the modeled estuary by van Dijk et al. (2021) disallowed for bank erosion compared to the experimental setup in this study. Therefore, the total channel length to be dredged increased in the experimental setup and is probably partly responsible for the increasing dredging volumes.

In our experiments, one of the most notable outcomes is the very clear meandering that occurs in the experiment with dredging and sea-level rise (Figures 2 and 7). Dredging removes bed level irregularities in the main channel and causes flow to concentrate in the main channels. This leads to a change in flow velocity and sediment transport in our experiments, in consonance with the work of Nichols (2018). This trend is in line with previous findings in models/case studies (Grasmeijer & van Weerdenburg, 2020; van Til, 2018). In case of the experiment with SLR and dredging, tidal flow in the upstream half of the estuary is focused in a single meandering channel that conveys the flow momentum, whilst the intertidal areas mainly seem to act as intertidal storage areas, conforming to 1D modeling of estuaries (Friedrichs & Aubrey, 1994). Consequently, the focused flow maintains active morphodynamics also in the upstream half of the estuary and causes ongoing lateral migration of the meandering bends.

Expansion of channel bends increases shipping fairway length, and consequently maintenance dredging volumes, something observed in the navigation channels of the Wadden Sea (van Til, 2018) (Figure 7). In the Wadden Sea, dredged channels have a meander extent/average sinuosity 10% larger than naturally formed channels (Grasmeijer & van Weerdenburg, 2020; van Til, 2018) (Figure 7). In our experiments (see Table 2), this difference ranges from 1% to 12% without SLR and 6%–15% with SLR. We identify that SLR in the absence of dredging can actually decrease or stabilize channel sinuosity. The combined effects of dredging and SLR however, cause a significant increase in sinuosity, which is amplified as SLR increases, even after dredging has ceased.

We also identify that SLR will render channel deepening activities ineffective. The additional sediment due to SLR quickly infills the dredged/deepened channels in the mouth area. Channel deepening invariably leads to increased dredging volumes, for example, 2019 channel deepening in the Rhine-Meuse (Cox, Huismans, et al., 2021). Meanwhile, SLR is predicted to decrease friction and therefore slow down erosion (Wachler

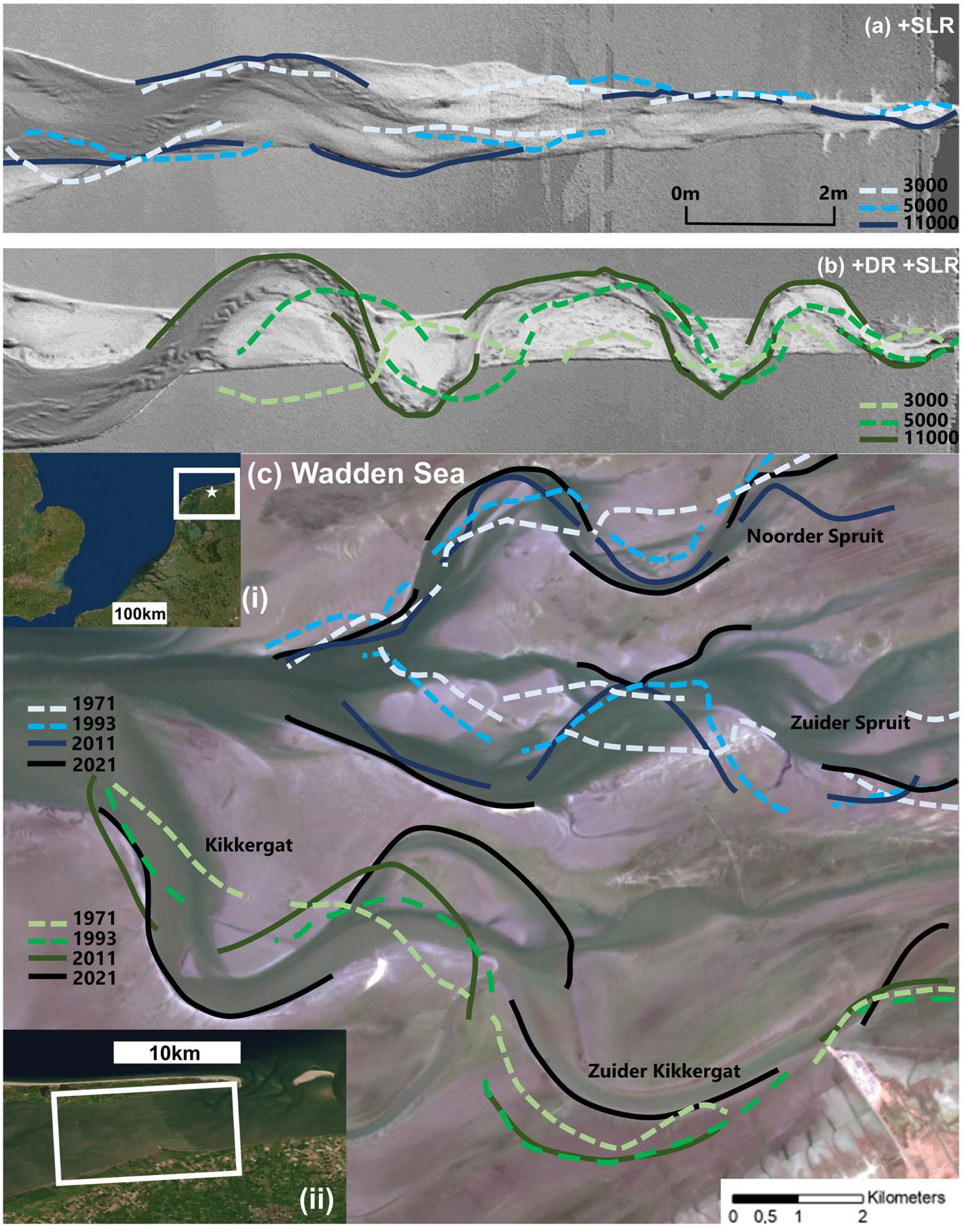

Figure 7. Comparison of meander bend migration in dredged and undredged channels in (a) the SLR only experiment, (b) the sea-level rise and dredging experiment and in (c) two real world channel networks in the Wadden Sea. The Kikkergat and Zuider Kikkergat channel are dredged for shipping and the Noorder and Zuider Spruit channels are undredged. Background map Planet Team (2021). Inset (i) shows the location of the Wadden Sea in the Netherlands. Inset (ii) shows the relative scale of the channels and position relative to the sea.

et al., 2020), something we see in the downstream parts of our SLR experiments (deltas gain elevation rapidly). This matches the predictions of Leuven et al. (2019) that in the mouth area where width is constrained and sediment supply is limited, channels become shallower and bars become subdued. It is possible that a certain threshold depth exists to balance the effects of SLR and channel deepening, but this hypothesis and potential threshold depth that balances sedimentation and erosion with dredging requirements needs to be further explored.

Table 2
Comparison of Sinuosity of the Main Channel in All Experiments, Where Numbers in Brackets Indicate the Percentage Difference in Sinuosity Relative to the Natural Experiment (No Dredging, No SLR)

Cycle number	Natural	+DR	+SLR	+DR + SLR
3000	1.06	1.07 (+1%)	1.11 (+6%)	1.12 (+6%)
5000	1.11	1.25 (+12%)	1.09 (−3%)	1.22 (+10%)
11,000	1.15	1.17 (+2%)	1.15 (0%)	1.32 (+15%)

Dredging and dumping activities hinder the creation of chute and connecting channels (third order channels that transverse intertidal areas providing sediment and water to all parts of the estuary system), which form as water levels in the main channel rise and spill over into adjacent intertidal areas. This was both observed in our experiments (see Figure 2) and in the Western Scheldt (Jeuken & Wang, 2010; van Dijk et al., 2021).

The channels in our SLR experiments increase in cross-sectional area as the tidal prism increases, in agreement with the proposition of Stefanon et al. (2012) wherein channel cross sections expand in response to the change in tidal prism caused by SLR. In the experiments of Stefanon et al. (2012), increased tidal prism causes erosion of the lagoonal bottom and expansion of the channel network; while the reduction in the tidal prism leads to a restored cross-sectional area due to infill and channel network contraction. We see a similar response in our experiments and in the PA relations.

The increase in tidal prism inland also increases sediment transport inland in our experiments, leading to increased dredging requirements inland/upstream. This matches the prediction of (Khojasteh et al., 2020) that tidal effects will be observed further inland. This is also reflected in the creation and sustenance of more upstream intertidal areas (shoals and bars) due to the change in tidal range. In systems like the Rhine-Meuse and Western Scheldt, where ports are located inland, this will become an important consideration for navigation, as channels tend to be narrower and more meandering further inland (e.g., near the cities of Rotterdam and Antwerp).

4.3. Implications of Changes to Estuary Morphology

Our experiments show that non-dredged systems will actually drown quicker than dredged systems (see Figure 5). This is due to the interaction of: (a) distribution of elevations, (b) channel network patterns, and (c) friction. Dredged estuary morphology tends to show large differences in elevations and channel depths, with high intertidal and supratidal areas (enforced by dumping of sediment) and deep channels. The dredging and dumping processes also decrease the number of connecting channels and side channels, disconnecting the pathways of water and sediment between the deep channel and surrounding areas. The higher and often unevenly elevated surrounding areas also enhance friction and slow down the tidal wave. These three factors combine to slow down the conveyance of water and sediment over the entire estuary and thus slow down the drowning of the estuary.

Undredged estuaries with shallow multichannel systems convey the additional water relatively evenly during ebb and flood, which can advance onto and drown intertidal areas. They have more subdued morphology (as proposed in Leuven et al. (2019)) with lower surrounding areas and shallower channels. The presence of connecting and side channels redistributes water and sediment evenly over the estuary.

Drowning and loss of intertidal areas is a key aspect of estuary management. Intertidal areas provide flood protection (Menéndez et al., 2020; Vuik et al., 2019) and are home to a great diversity of plants and animal life (Elliott et al., 2019; Kennish, 2002) that are instrumental in determining morphology (Brückner et al., 2019) and the elevation of these intertidal areas (Kakeh et al., 2016). The equilibrium of intertidal areas is placed at risk when bends aggressively migrate (Fagherazzi et al., 2013; van Dijk et al., 2019), as occurred when SLR and dredging interacted in our experiments. The disconnection and loss of intertidal area due to rising sea-levels is identified as a major issue (Rayner et al., 2021; Xie et al., 2020) in estuary and delta studies, particularly when intertidal areas are commonly identified as key regions for SLR mitigation (Luisetti et al., 2014; Timmerman et al., 2021). Our experiments indicate that SLR can provide an opportunity to reconnect and restore intertidal areas in dredged systems, as was previously shown by Kirwan et al. (2016); Leuven et al. (2019); van Dijk et al. (2021).

The change to fairway length due to meander expansion is an important aspect of transport infrastructure, port competitiveness and efficiency (Zhou et al., 2014). In the Wadden Sea, a new channel was cut through a flood chute to shorten the journey of ships (Grasmeijer & van Weerdenburg, 2020). However, this solution is not possible in most urban deltas and estuaries, as most channels have already been historically straightened and surrounding land is extensively embanked. Moreover, it does not solve the issue of extensive erosion of dredged bends, unless dredging were to be reversed (i.e., channels shallowed), a suggested adaptation pathway for the Rhine-Meuse delta (Meyer, 2021). In our experiments, the halting of dredging and dumping activities does not

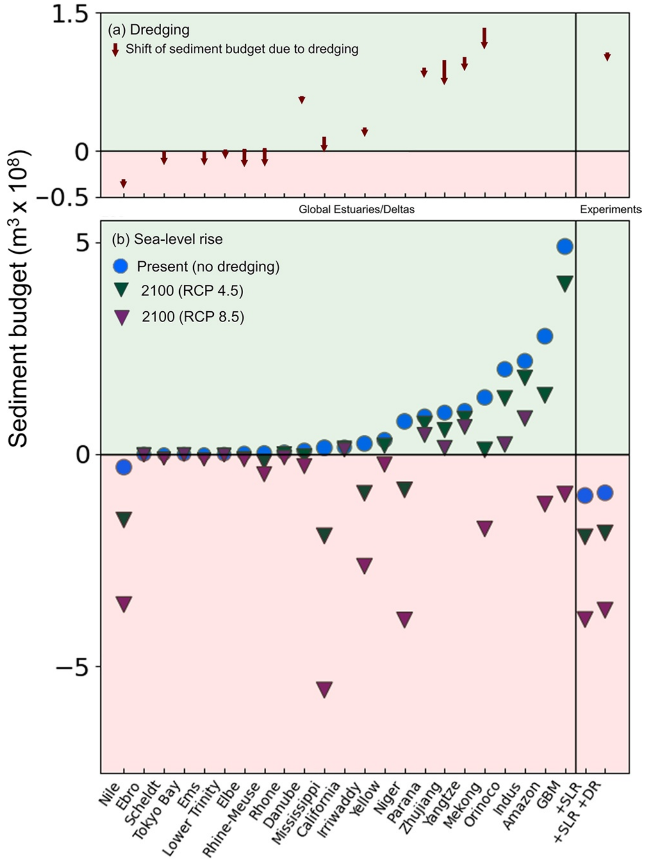

Figure 8. Sediment budget ($Q_{\text{river}} - Q_{\text{SLR}}$) change due to (a) dredging and (b) sea-level rise for a selection of global deltas and experiments. Experiments are scaled by $\times 10^9$ (making experiment estuary area 60,000 km^2, while the selection of systems compared in the figure range in size from 12 km^2 to 70,000 km^2) for inclusion on the figure (and SLR RCP4.5 = 4 mm SLR, and RCP 8.5 is 8 mm SLR for the experiments). GBM is the Ganges-Brahmaputra Meghna delta and Tokyo Bay refers to the Arakawa/Tama-gawa estuary mouths. The shift due to dredging combines the present sediment budget (as calculated from Nienhuis and van de Wal (2021)) with reported annual maintenance dredging estimates for each system taken from Anthony et al. (2019); Arnaud-Fassetta (2003); Cox, Huismans, et al. (2021); Frey and Coe (2020); Frihy et al. (2015); Habersack et al. (2016); Jordan et al. (2019); Kemp et al. (2014); Liu and Zhang (2019); Marineau and Wright (2015); Rudra (2014); Smets et al. (1997); van Dijk et al. (2021); van Maren et al. (2015); Weilbeer (2014); Wu et al. (2018). Data concerning present sediment budgets and predicted sediment loss due to SLR are from Nienhuis and van de Wal (2021).

automatically allow the system to revert back to a "natural state"; the inherited morphology will continue to persist.

In many cases, where estuaries and channels have become fixed, the tendency for meandering will be experienced as excess energy and pressure being placed on outer bends of channels or in a vertical direction (bed erosion). This means that existing protection structures (embankments, dikes etc.) will be placed under pressure. Moreover, increased water levels in the channels will also put pressure on the heights and strengths of flood control measures like storm surge barriers, which in the Netherlands for example, are built for 1 m of SLR or until 2100 (Nillesen et al., 2021).

4.4. Estuaries and Deltas at Risk

Figure 8 shows the impact of dredging and SLR on the sediment budgets of global estuary and delta systems compared with the experiments. Figure 8a indicates that in many cases, annual maintenance dredging is shifting sediment budgets from positive to negative. This is particularly true for systems which already have a small-scale sediment budget (from −1 to 1 Mt/yr), that is, many European estuaries and deltas. As shown in Cox, Huismans, et al. (2021) and Cox et al. (2022), and as reported here, many estuaries and deltas in Europe which are home to ports currently undertake extensive dredging, including the Rhine-Meuse (the Netherlands), Western Scheldt (the Netherlands), Ems-Dollard (the Netherlands/Germany) Seine (France), Loire (France), Elbe (Germany) and Danube delta (Romania). They also have a typically small area and low river sediment flux (see Figure 8 and Data Set S1). Therefore, extensive dredging activities can cause a significant shift in their sediment budgets, often from stable (around 0) or slightly positive to negative. In the case of these small to mid-size deltas, estuaries and bays, dredging is far more significant in altering sediment budgets than SLR. Thus, the primary concern in terms of morphology revolves around sediment management.

Meanwhile larger deltas and estuaries (such as those in China) continue to have a positive budget despite dredging. This is linked mostly to their high riverine sediment delivery (Dunn et al., 2019; Nienhuis & van de Wal, 2021). Many of the world's large deltas (Mississippi, Yellow, Niger, Parana, Zhujiang/Pearl, Yangtze, Mekong, Orinoco, Indus, Amazon, Ganges-Brahmaputra Meghna) can easily accommodate dredging, but SLR will be the major challenge in terms of sediment budget and rate of drowning. In the case of our experiments, dredging does not shift the sediment budget from positive to negative and indeed, our dredging volumes are quite modest compared to many of the world's deltas when scaled (though we recognize our scaling method is an over simplification; see Figure 8).

This conclusion fits with our observations from the experiments that undredged systems can drown more quickly and lose intertidal area more quickly due to SLR. Many of the large Asian deltas show multichannel systems akin to natural systems (e.g., the Ganges-Brahmaputra Meghna, Mekong) which convey water quickly into surrounding plains. Meanwhile, the new equilibrium set up by dredging that is, a deep single channel disconnected from elevated and high friction plains, has uneven conveyance of water and takes longer to drown entirely.

5. Conclusions

Many urban deltas and estuaries are being dredged for access to ports and harbors. This process has set up a new typical equilibrium with a deep dredged main channel and intertidal areas which are disconnected from this main channel and therefore flows of water and sediment. Sea level rise (SLR) interacts with dredging by (a) increasing the spatial area that requires dredging, (b) increasing dredging volumes, (c) shifting dredging locations upstream, and (d) making channel deepening events ineffective. SLR causes enhanced meandering in dredged channels, which manifests itself in fixed systems as excess energy and pressure on river beds and banks, placing flood safety infrastructure and risk. In systems with low sediment availability on the bed (such as due to geological constraints), this excess energy exacerbates bank failure risk.

SLR can reconnect dredged channels with intertidal areas and slow down drowning; meanwhile natural systems will rapidly drown without intervention (activities which raise land/reduce land loss due to SLR). Therefore, solutions which reconnect systems to their intertidal areas and enhance accretion in these zones to keep up with SLR must be pursued to provide extra time and capacity to grow with SLR. The capacity to introduce these solutions is, in practice, limited by available space and policy, legal and social constraints. Moreover, the shallowing of dredged channels, which will naturally occur with SLR (as enhanced sediment import at the seaward boundary causes additional deposition in deep dredged channels), may provide useful flood protection, as the additional sediment can become a natural protection for channel banks and river beds.

Different estuaries and deltas globally will face different key challenges in terms of their land loss and sediment budget. Large Asian deltas are more at risk from SLR, while midsize European deltas are mainly at risk of drowning due to excessive dredging.

Data Availability Statement

Additional materials are provided in an online database (Cox, 2022): available at https://doi.org/10.24416/UU01-CZM7SV. It provides the digital elevation models of the four experiments and the input and output files of the hydrodynamic modelling in Nays2D. Data Set S1 includes the global delta land loss and dredging volumes based on literature. For installation and using the hydrodynamic model Nays2D, the reader is referred to Weisscher (2020). The network tool that was used to extract the channel centerlines is called TTGA: Topological Tools for Geomorphological Analysis (Sonke, 2020) and is available at https://doi.org/10.5281/zenodo.3634684.

Acknowledgments
Funding this research was supported by the research program Rivers2Morrow (2018–2023). Rivers2Morrow is financed by the Dutch Ministry of Infrastructure and Water Management. This work is part of the PhD projects of Jana Cox and Steven Weisscher. Steven Weisscher and Maarten Kleinhans were supported by the European Research Council through the ERC Consolidator Grant 647570 awarded to Kleinhans. We are grateful for the support of the Metronome technical staff and Jan-Eike Rossius for their assistance in carrying out experiments. We thank Jaap Nienhuis for providing global delta land loss data and consultation on this topic. We thank Jelmer Cleveringa for insightful discussions and information concerning the field case in the Wadden Sea. We are grateful for the comments from Bas van Maren, Mikael Attal, and one anonymous reviewer that helped to improve the manuscript.

References

Anthony, E. J., Besset, M., Dussouillez, P., Goichot, M., & Loisel, H. (2019). Overview of the Monsoon-influenced Ayeyarwady river delta, and delta shoreline mobility in response to changing fluvial sediment supply. *Marine Geology*, *417*, 106038. https://doi.org/10.1016/j.margeo.2019.106038

Arnaud-Fassetta, G. (2003). River channel changes in the Rhone delta (France) since the end of the little Ice Age: Geomorphological adjustment to hydroclimatic change and natural resource management. *Catena*, *51*(2), 141–172. https://doi.org/10.1016/s0341-8162(02)00093-0

Bendixen, M., Best, J., Hackney, C., & Iversen, L. L. (2019). Time is running out for sand. *Nature*, *571*, 29–31. https://doi.org/10.1038/d41586-019-02042-4

Braat, L., Leuven, J. R., Lokhorst, I. R., & Kleinhans, M. G. (2019). Effects of estuarine mudflat formation on tidal prism and large-scale morphology in experiments. *Earth Surface Processes and Landforms*, *44*(2), 417–432. https://doi.org/10.1002/esp.4504

Braat, L., van Kessel, T., Leuven, J. R., & Kleinhans, M. G. (2017). Effects of mud supply on large-scale estuary morphology and development over centuries to millennia. *Earth Surface Dynamics*, *5*(4), 617–652. https://doi.org/10.5194/esurf-5-617-2017

Brückner, M. Z., Schwarz, C., van Dijk, W. M., van Oorschot, M., Douma, H., & Kleinhans, M. G. (2019). Salt marsh establishment and eco-engineering effects in dynamic estuaries determined by species growth and mortality. *Journal of Geophysical Research: Earth Surface*, *124*(12), 2962–2986. https://doi.org/10.1029/2019JF005092

Burchard, H., Schuttelaars, H. M., & Ralston, D. K. (2018). Sediment trapping in estuaries. *Annual Review of Marine Science*, *10*, 371–395. https://doi.org/10.1146/annurev-marine-010816-060535

Cai, H., Savenije, H. H., & Toffolon, M. (2012). A new analytical framework for assessing the effect of sea-level rise and dredging on tidal damping in estuaries. *Journal of Geophysical Research*, *117*(C9), C09023. https://doi.org/10.1029/2012jc008000

Chen, W., Chen, K., Kuang, C., Zhu, D. Z., He, L., Mao, X., & Song, H., (2016). Influence of sea level rise on saline water intrusion in the Yangtze River Estuary, China. *Applied Ocean Research*, *54*, 12–25. https://doi.org/10.1016/j.apor.2015.11.002

Cox, J. R. (2022). Data supplement to effects of sea-level rise on dredging and dredged estuary morphology. YODA [Dataset]. https://doi.org/10.24416/UU01-CZM7SV

Cox, J. R., Dunn, F., Nienhuis, J., van der Perk, M., & Kleinhans, M. (2021). Climate change and human influences on sediment fluxes and the sediment budget of an urban delta: The example of the lower rhine–Meuse delta distributary network. *Anthropocene Coasts*, *4*(1), 251–280. https://doi.org/10.1139/anc-2021-0003

Cox, J. R., Huismans, Y., Knaake, S., Leuven, J. R., Vellinga, N., van der Vegt, M., & Kleinhans, M. (2021). Anthropogenic effects on the contemporary sediment budget of the lower Rhine-Meuse Delta channel network. *Earth's Future*, 9(7), e2020EF001869.

Cox, J. R., Leuven, J. R., Pierik, H., van Egmond, M., & Kleinhans, M. (2022). Sediment deficit and morphological change of the Rhine-Meuse river mouth attributed to multi-millennial anthropogenic impacts. *Continental Shelf Research*, 104766. https://doi.org/10.1016/j.csr.2022.104766

De Vriend, H. J., Wang, Z. B., Ysebaert, T., Herman, P. M., & Ding, P. (2011). Eco-morphological problems in the yangtze estuary and the Western Scheldt. *Wetlands*, *31*(6), 1033–1042. https://doi.org/10.1007/s13157-011-0239-7

Dunn, F. E., Darby, S. E., Nicholls, R. J., Cohen, S., Zarfl, C., & Fekete, B. M. (2019). Projections of declining fluvial sediment delivery to major deltas worldwide in response to climate change and anthropogenic stress. *Environmental Research Letters*, *14*(8), 084034. https://doi.org/10.1088/1748-9326/ab304e

Dunn, F. E., & Minderhoud, P. S. (2022). Sedimentation strategies provide effective but limited mitigation of relative sea-level rise in the Mekong delta. *Communications Earth & Environment*, *3*(1), 1–12. https://doi.org/10.1038/s43247-021-00331-3

Elliott, M., Day, J. W., Ramachandran, R., & Wolanski, E. (2019). A synthesis: What is the future for coasts, estuaries, deltas and other transitional habitats in 2050 and beyond? In *Coasts and estuaries* (pp. 1–28). Oxford: Elsevier. https://doi.org/10.1016/b978-0-12-814003-1.00001-0

Fagherazzi, S., Mariotti, G., Wiberg, P. L., & McGlathery, K. J. (2013). Marsh collapse does not require sea level rise. *Oceanography*, *26*(3), 70–77. https://doi.org/10.5670/oceanog.2013.47

Frey, A. E., & Coe, L. A. (2020). *Effect of tropical storms and precipitation on dredging volumes*:Houston-Galveston, TX, and Mayport, FL.

Friedrichs, C. T., & Aubrey, D. G. (1994). Tidal propagation in strongly convergent channels. *Journal of Geophysical Research*, *99*(C2), 3321–3336. https://doi.org/10.1029/93jc03219

Frihy, O., Deabes, E., Moufaddal, W., & El-Shahat, A. (2015). Recycling of coastal dredged sediments from the northern Nile Delta, Egypt, for heavy minerals exploitation. *Marine Georesources & Geotechnology*, *33*(5), 408–418. https://doi.org/10.1080/1064119x.2014.920284

Grasmeijer, B., & van Weerdenburg, R. (2020). Evaluatie Bochtafsnijding Vaarweg Ameland. Deltares Rapport. Retrieved from https://publicwiki.deltares.nl/download/attachments/137135283/11205229-006-ZKS-0002_v1.1-Evaluatie\Bochtafsnijding\Vaarweg\Ameland\-\.pdf?version=1&modificationDate=1607942377903&api=v2

Habersack, H., Hein, T., Stanica, A., Liska, I., Mair, R., Jäger, E., et al. (2016). Challenges of river basin management: Current status of, and prospects for, the River Danube from a river engineering perspective. *Science of the Total Environment*, *543*, 828–845. https://doi.org/10.1016/j.scitotenv.2015.10.123

Hijma, M. P., & Cohen, K. M. (2011). Holocene transgression of the Rhine river mouth area, The Netherlands/Southern North sea: Palaeogeography and sequence stratigraphy. *Sedimentology*, *58*(6), 1453–1485. https://doi.org/10.1111/j.1365-3091.2010.01222.x

Hill, C., Dunn, F., Haque, A., Amoako-Johnson, F., Nicholls, R. J., Raju, P. V., & Addo, K. A. (2020). Hotspots of present and future risk within deltas: Hazards, Exposure and Vulnerability. In *Deltas in the anthropocene* (pp. 127–151). Palgrave Macmillan. https://doi.org/10.1007/978-3-030-23517-8_6

Hoitink, A., Wang, Z. B., Vermeulen, B., Huismans, Y., & Kästner, K. (2017). Tidal controls on river delta morphology. *Nature Geoscience*, *10*(9), 637–645. https://doi.org/10.1038/ngeo3000

Hong, B., Liu, Z., Shen, J., Wu, H., Gong, W., Xu, H., & Wang, D. (2020). Potential physical impacts of sea-level rise on the Pearl River Estuary, China. *Journal of Marine Systems*, *201*, 103245. https://doi.org/10.1016/j.jmarsys.2019.103245

Hong, B., & Shen, J. (2012). Responses of estuarine salinity and transport processes to potential future sea-level rise in the Chesapeake Bay. Estuarine. *Coastal and Shelf Science*, *104*, 33–45. https://doi.org/10.1016/j.ecss.2012.03.014

Ibáñez, C., Day, J. W., & Reyes, E. (2014). The response of deltas to sea-level rise: Natural mechanisms and management options to adapt to high-end scenarios. *Ecological Engineering*, *65*, 122–130.

Jarrett, J. T. (1976). US Army Engineer Waterways Experiment station. In *Tidal Prism: Inlet Area Relationships* (Vol. *3*).

Jeuken, M., & Wang, Z. (2010). Impact of dredging and dumping on the stability of ebb–flood channel systems. *Coastal Engineering*, *57*(6), 553–566. https://doi.org/10.1016/j.coastaleng.2009.12.004

Jordan, C., Tiede, J., Lojek, O., Visscher, J., Apel, H., Nguyen, H. Q., et al. (2019). Sand mining in the Mekong Delta revisited-current scales of local sediment deficits. *Scientific Reports*, *9*(1), 1–14. https://doi.org/10.1038/s41598-019-53804-z

Kakeh, N., Coco, G., & Marani, M. (2016). On the morphodynamic stability of intertidal environments and the role of vegetation. *Advances in Water Resources*, *93*, 303–314. https://doi.org/10.1016/j.advwatres.2015.11.003

Kemp, G. P., Day, J. W., & Freeman, A. M. (2014). Restoring the sustainability of the Mississippi river delta. *Ecological Engineering*, *65*, 131–146. https://doi.org/10.1016/j.ecoleng.2013.09.055

Kennish, M. J. (2002). Environmental threats and environmental future of estuaries. *Environmental Conservation*, *29*(1), 78–107. https://doi.org/10.1017/s0376892902000061

Khojasteh, D., Glamore, W., Heimhuber, V., & Felder, S. (2021). Sea level rise impacts on estuarine dynamics: A review. *Science of the Total Environment*, *780*, 146470. https://doi.org/10.1016/j.scitotenv.2021.146470

Khojasteh, D., Hottinger, S., Felder, S., De Cesare, G., Heimhuber, V., Hanslow, D. J., & Glamore, W. (2020). Estuarine tidal response to sea level rise: The significance of entrance restriction. *Estuarine, Coastal and Shelf Science*, *244*, 106941. https://doi.org/10.1016/j.ecss.2020.106941

Kirwan, M. L., Temmerman, S., Skeehan, E. E., Guntenspergen, G. R., & Fagherazzi, S. (2016). Overestimation of marsh vulnerability to sea level rise. *Nature Climate Change*, *6*(3), 253–260. https://doi.org/10.1038/nclimate2909

Kleinhans, M. G. (2010). Sorting out river channel patterns. *Progress in Physical Geography*, *34*(3), 287–326. https://doi.org/10.1177/0309133310365300

Kleinhans, M. G., Roelofs, L., Weisscher, S. A. H., Lokhorst, I. R., & Braat, L. (2022). Estuarine morphodynamics and development modified by floodplain formation. *Earth Surface Dynamics*, *10*(2), 367–381. https://doi.org/10.5194/esurf-10-367-2022

Kleinhans, M. G., van der Vegt, M., Leuven, J. R., Braat, L., Markies, H., Simmelink, A., et al. (2017). Turning the tide: Comparison of tidal flow by periodic sea level fluctuation and by periodic bed tilting in scaled landscape experiments of estuaries. *Earth Surface Dynamics*, *5*(4), 731–756. https://doi.org/10.5194/esurf-5-731-2017

Kleinhans, M. G., van Scheltinga, R. T., van der Vegt, M., & Markies, H. (2015). Turning the tide: Growth and dynamics of a tidal basin and inlet in experiments. *Journal of Geophysical Research: Earth Surface*, *120*(1), 95–119. https://doi.org/10.1002/2014jf003127

KNMI. (2021). KNMI Klimaatsignaal'21: Hoe het klimaat in Nederland SNEL verandert (pp. 1–72).

Leuven, J. R., Braat, L., van Dijk, W. M., de Haas, T., van Onselen, E., Ruessink, B., & Kleinhans, M. G. (2018). Growing forced bars determine nonideal estuary planform. *Journal of Geophysical Research: Earth Surface*, *123*(11), 2971–2992. https://doi.org/10.1029/2018jf004718

Leuven, J. R., De Haas, T., Braat, L., & Kleinhans, M. G. (2018). Topographic forcing of tidal sandbar patterns for irregular estuary planforms. *Earth Surface Processes and Landforms*, *43*(1), 172–186. https://doi.org/10.1002/esp.4166

Leuven, J. R., Kleinhans, M., Weisscher, S., & van der Vegt, M. (2016). Tidal sand bar dimensions and shapes in estuaries. *Earth-Science Reviews*, *161*, 204–223. https://doi.org/10.1016/j.earscirev.2016.08.004

Leuven, J. R., Pierik, H. J., van der Vegt, M., Bouma, T. J., & Kleinhans, M. G. (2019). Sea-level-rise-induced threats depend on the size of tide-influenced estuaries worldwide. *Nature Climate Change*, *9*(12), 986–992. https://doi.org/10.1038/s41558-019-0608-4

Leuven, J. R., van Maanen, B., Lexmond, B. R., van der Hoek, B. V., Spruijt, M. J., & Kleinhans, M. G. (2018). Dimensions of fluvial-tidal meanders: Are they disproportionally large? *Geology*, *46*(10), 923–926. https://doi.org/10.1130/g45144.1

Liu, M., & Zhang, H.-W. (2019). Correction of the artificial influence on dredging volume in the Yangtze estuary deep-water channel. *IOP Conference Series: Earth and Environmental Science*, *304*, 022004. https://doi.org/10.1088/1755-1315/304/2/022004

Loucks, D. P. (2019). Developed river deltas: Are they sustainable? *Environmental Research Letters*, *14*(11), 113004. https://doi.org/10.1088/1748-9326/ab4165

Luisetti, T., Turner, R., Jickells, T., Andrews, J., Elliott, M., Schaafsma, M., et al. (2014). Coastal zone ecosystem services: From science to values and decision making; a case study. *Science of the Total Environment*, *493*, 682–693. https://doi.org/10.1016/j.scitotenv.2014.05.099

Maes, F., De Batist, M., van Lancker, V., Leroy, D., & Vincx, M. (2005). Towards a spatial structure plan for sustainable management of the sea: Mixed actions-final report: SPSD II (MA/02/006).

Marineau, M. D., & Wright, S. A. (2015). Effects of human alterations on the hydrodynamics and sediment transport in the Sacramento-San Joaquin Delta, California. *Proceedings of the International Association of Hydrological Sciences*, *367*, 399–406. https://doi.org/10.5194/piahs-367-399-2015

Masson-Delmotte, V., Zhai, P., Pirani, A., Connors, S. L., Péan, C., Berger, S., et al. (2021). Climate change 2021: The Physical Science Basis. *Contribution of Working Group I to the Sixth Assessment Report of the Intergovernmental Panel on Climate Change*. Geneva, Switzerland:IPCC.

Mayor-Mora, R. E. (1977). *Laboratory investigation of tidal inlets on sandy coasts (Tech. Rep. No. ADA040021)*. California University, Berkeley Hydraulic Engineering Laboratory.

Menéndez, P., Losada, I. J., Torres-Ortega, S., Narayan, S., & Beck, M. W. (2020). The global flood protection benefits of mangroves. *Scientific Reports*, *10*(1), 1–11.

Meyer, H. (2021). *De Rijnmonding als estuarium*. ARK Nature Development. Retrieved from https://www.ark.eu/sites/default/files/media/Rijnmonding_als_estuarium.pdf

Monge-Ganuzas, M., Cearreta, A., & Evans, G. (2013). Morphodynamic consequences of dredging and dumping activities along the lower Oka estuary (Urdaibai Biosphere Reserve, southeastern Bay of Biscay, Spain). *Ocean & Coastal Management*, *77*, 40–49. https://doi.org/10.1016/j.ocecoaman.2012.02.006

Nicholls, R. J., Adger, W. N., Hutton, C. W., & Hanson, S. E. (2020). Delta challenges and trade-offs from the Holocene to the anthropocene. *Deltas in the Anthropocene*, *1–22*. https://doi.org/10.1007/978-3-030-23517-8_1

Nichols, M. M. (2018). Consequences of dredging. In *Hydrodynamics of Estuaries*, (Vol. 462). CRC Press.

Nienhuis, J. H., & van de Wal, R. S. (2021). Projections of global delta land loss from sea-level rise in the 21st century. *Geophysical Research Letters*, *48*(14), e2021GL093368. https://doi.org/10.1029/2021gl093368

Niesten, I., Hoitink, T., Vermeulen, B., Huismans, Y., & EGU21 (2021). Mixed sediment transport in a stratified estuary: First insights from a field study. *Paper presented at EGU General Assembly Conference Abstracts, EGU21-14362*.

Nillesen, A. L., zum Felde, M., & Lijdsman, L. (2021). *Versnelde zeespiegelstijging in Rijnmond-Drechtsteden*. Defacto stedenbouw.

O'Brien, M. P. (1931). Estuary tidal prisms related to entrance areas. *Civil Engineering* (Vol. *1*(8), pp. 738–739).

O'Brien, M. P. (1969). Equilibrium flow areas of inlets on sandy coasts. *Journal of the Waterways and Harbors Division*, *95*(1), 43–52.

O'Dell, J., Nienhuis, J. H., Cox, J. R., Edmonds, D. A., & Scussolini, P. (2021). A global open-source database of flood-protection levees on river deltas (openDELvE). *Natural Hazards and Earth System Sciences Discussions*, *2021*, 1–16. Retrieved from https://nhess.copernicus.org/preprints/nhess-2021-291/

Pierik, H. J., Leuven, J. R., Busschers, F. S., Hijma, M. P., & Kleinhans, M. G. (2022). Depth-limiting resistant layers restrict dimensions and positions of estuarine channels and bars. *The Depositional Record*.

Planet Team. (2021). Planet Application Program Interface: In Space for Life on Earth. San Francisco, CA.Retrieved from https://api.planet.com

Rayner, D., Glamore, W., Grandquist, L., Ruprecht, J., Waddington, K., & Khojasteh, D. (2021). Intertidal wetland vegetation dynamics under rising sea levels. *Science of the Total Environment*, *766*, 144237. https://doi.org/10.1016/j.scitotenv.2020.144237

Rudra, K. (2014). Changing river courses in the Western part of the Ganga–Brahmaputra delta. *Geomorphology*, *227*, 87–100. https://doi.org/10.1016/j.geomorph.2014.05.013

Rust, B. R. (1977). A classification of alluvial channel systems.

Savenije, H. H. (2005). *Salinity and tides in alluvial estuaries*. Gulf Professional Publishing.

Seabergh, W. C., King, D. B., & Stephens, B. E. (2001). *Tidal Inlet Equilibrium Area Experiments, Inlet Laboratory Investigations*,US Army Corps of Engineers, Engineer Research and Development Center (Vol. *1*).

Shimozono, T., Tajima, Y., Akamatsu, S., Matsuba, Y., & Kawasaki, A. (2019). Large-scale channel migration in the Sittang river estuary. *Scientific Reports*, *9*(1), 1–9. https://doi.org/10.1038/s41598-019-46300-x

Smets, V., Jacobs, B., & Catteau, P. (1997). The Martin Garcia channel project. *Terra et Aqua (English Edition)*.

Sonke, W. (2020). TTGA: Topological tools for geomorphological analysis. tueaga/ttga:. [Dataset]. https://doi.org/10.5281/zenodo.3634684

Sonke, W., Speckmann, B., Kleinhans, M., van Dijk, W., & Hiatt, M. (2022). Alluvial connectivity in multi-channel networks in rivers and estuaries. *Earth Surface Processes and Landforms*, *47*(2), 477–490. https://doi.org/10.1002/esp.5261

Stefanon, L., Carniello, L., D'Alpaos, A., & Lanzoni, S. (2010). Experimental analysis of tidal network growth and development. *Continental Shelf Research*, *30*(8), 950–962. https://doi.org/10.1016/j.csr.2009.08.018

Stefanon, L., Carniello, L., D'Alpaos, A., & Rinaldo, A. (2012). Signatures of sea level changes on tidal geomorphology: Experiments on network incision and retreat. *Geophysical Research Letters*, *39*(12). https://doi.org/10.1029/2012gl051953

Steijn, R., Cleveringa, J., Leuven, J. R., Baan, J., & van der Zanden, J. (2019). Extreme coastal dynamics of Sittaung estuary (Myanmar). In *International Conference on Asian and Pacific Coasts* (pp. 1193–1200). https://doi.org/10.1007/978-981-15-0291-0_163

Talke, S. A., & Jay, D. A. (2020). Changing tides: The role of natural and anthropogenic factors. *Annual Review of Marine Science*, *12*, 121–151. https://doi.org/10.1146/annurev-marine-010419-010727

Temmerman, S., Meire, P., Bouma, T. J., Herman, P. M. J., Ysebaert, T., & de Vriend, H. J. (2013). Ecosystem-based coastal defence in the face of global change. *Nature*, *504*, 79–83. https://doi.org/10.1038/nature12859

Ten Brinke, W. B., Schulze, F. H., & van Der Veer, P. (2004). Sand exchange between groyne-field beaches and the navigation channel of the Dutch Rhine: The impact of navigation versus river flow. *River Research and Applications*, *20*(8), 899–928. https://doi.org/10.1002/rra.809

Timmerman, A., Haasnoot, M., Middelkoop, H., Bouma, T., & McEvoy, S. (2021). Ecological consequences of sea level rise and flood protection strategies in shallow coastal systems: A quick-scan barcoding approach. *Ocean & Coastal Management*, *210*, 105674. https://doi.org/10.1016/j.ocecoaman.2021.105674

van den Hurk, B., Siegmund, P., Klein-Tank, A., Attema, J., Bakker, A., Beersma, J., & van Zadelhof, G.-J. (2014). KNMI'14: Climate change scenarios for the 21st century-a Netherlands perspective. *KNMI WR-2014-01, 6–83*. Retrieved from http://publicaties.minienm.nl/documenten/knmi-14-climate-change-scenarios-for-the-21st-century-a-netherla van der Deijl, E. C., van der Perk, M., & Middelkoop, H. (2017). Factors controlling sediment trapping in two freshwater tidal wetlands in the Biesbosch area, The Netherlands. *Journal of Soils and Sediments*, *17*(11), 2620–2636. https://doi.org/10.1007/s11368-017-1729-x

van Dijk, W. M., Cox, J. R., Leuven, J. R., Cleveringa, J., Taal, M., Hiatt, M. R., & Kleinhans, M. G. (2021). The vulnerability of tidal flats and multi-channel estuaries to dredging and disposal. *Anthropocene Coasts*, *4*(1), 36–60. https://doi.org/10.1139/anc-2020-0006

van Dijk, W. M., Hiatt, M., van der Werf, J., & Kleinhans, M. G. (2019). Effects of shoal margin collapses on the morphodynamics of a sandy estuary. *Journal of Geophysical Research: Earth Surface*, *124*(1), 195–215. https://doi.org/10.1029/2018JF004763

van Maren, D., van Kessel, T., Cronin, K., & Sittoni, L. (2015). The impact of channel deepening and dredging on estuarine sediment concentration. *Continental Shelf Research*, *95*, 1–14. https://doi.org/10.1016/j.csr.2014.12.010

van Til, S. (2018). Getijdemeanders in Kombergingsgebied Borndiep. Arcadis Rapport. Retrieved from https://publicwiki.deltares.nl/download/attachments/137135283/C03011_000539_Getijdemeanders_in_kombergingsgebied_borndiep_20180928_rapport_2018.pdf?version=1%26modificationDate=1547545427337%26api=v2

van Veen, J., van der Spek, A. J., Stive, M. J., & Zitman, T. (2005). Ebb and flood channel systems in The Netherlands tidal waters. *Journal of Coastal Research*, *21*(6), 1107–1120. https://doi.org/10.2112/04-0394.1

van Wesenbeeck, B. K., Mulder, J. P., Marchand, M., Reed, D. J., de Vries, M. B., de Vriend, H. J., & Herman, P. M. (2014). Damming deltas: A practice of the past? Towards nature-based flood defenses. *Estuarine, Coastal and Shelf Science*, *140*, 1–6. https://doi.org/10.1016/j.ecss.2013.12.031

Vellinga, N., Hoitink, A., van der Vegt, M., Zhang, W., & Hoekstra, P. (2014). Human impacts on tides overwhelm the effect of sea level rise on extreme water levels in the Rhine–Meuse delta. *Coastal Engineering*, *90*, 40–50. https://doi.org/10.1016/j.coastaleng.2014.04.005

Vuik, V., Borsje, B. W., Willemsen, P. W., & Jonkman, S. N. (2019). Salt marshes for flood risk reduction: Quantifying long-term effectiveness and life-cycle costs. *Ocean & Coastal Management*, *171*, 96–110. https://doi.org/10.1016/j.ocecoaman.2019.01.010

Wachler, B., Seiffert, R., Rasquin, C., & Kösters, F. (2020). Tidal response to sea level rise and bathymetric changes in the German Wadden Sea. *Ocean Dynamics*, *70*(8), 1033–1052. https://doi.org/10.1007/s10236-020-01383-3

Weilbeer, H. (2014). Sediment transport and sediment management in the Elbe estuary. *Die Kuste*, *IADC*(81), 409–426.

Weisscher, S. A. (2020). Data supplementary to complementing scale experiments of rivers and estuaries with numerically modelled hydrodynamics. YODA [Software]. [Dataset]. https://doi.org/10.24416/UU01-CZV56M

Weisscher, S. A., Boechat-Albernaz, M., Leuven, J. R., van Dijk, W. M., Shimizu, Y., & Kleinhans, M. G. (2020). Complementing scale experiments of rivers and estuaries with numerically modelled hydrodynamics. *Earth Surface Dynamics*, *8*(4), 955–972. https://doi.org/10.5194/esurf-8-955-2020

Weisscher, S. A., van den Hoven, K., Pierik, H. J., & Kleinhans, M. G., (2022). Building and raising land: Mud and vegetation effects in infilling estuaries. *Journal of Geophysical Research: Earth Surface*(1), 127. https://doi.org/10.1029/2021jf006298

White, E. D., Meselhe, E., Reed, D., Renfro, A., Snider, N. P., & Wang, Y. (2019). Mitigating the effects of sea-level rise on estuaries of the Mississippi Delta Plain using river diversions. *Water*, *11*(10), 2028. https://doi.org/10.3390/w11102028

Wong, P., Losada, I., Gattuso, J.-P., Hinkel, J., Khattabi, A., McInnes, K., & Sallenger, A. (2014). Coastal systems and low-lying areas. In *Climate change 2014: Impacts, adaptation, and vulnerability. Part A: Global and sectoral aspects. Contribution of working Group II to the fifth assessment report of the intergovernmental panel on climate change* (pp. 361–409). Cambridge University Press.

Wu, Z., Milliman, J. D., Zhao, D., Cao, Z., Zhou, J., & Zhou, C. (2018). Geomorphologic changes in the lower Pearl River Delta, 1850–2015, largely due to human activity. *Geomorphology*, *314*, 42–54. https://doi.org/10.1016/j.geomorph.2018.05.001

Xie, D., Schwarz, C., Brückner, M. Z., Kleinhans, M. G., Urrego, D. H., Zhou, Z., & van Maanen, B. (2020). Mangrove diversity loss under sea-level rise triggered by bio-morphodynamic feedbacks and anthropogenic pressures. *Environmental Research Letters*, *15*(11), 114033. https://doi.org/10.1088/1748-9326/abc122

Zhang, H., Ke, J., Dong, S., & Yuan, Z. (2019). Simulation modeling of state-dependent queuing network: Impact of deepening on the vessel traffic in yangtze river estuary. *Advances in Mechanical Engineering*, *11*(5), 1687814019845247. https://doi.org/10.1177/1687814019845247

Zhou, K., Dai, R., & Yue, X. (2014). Research on large-scale vessel riding tidal current to promote efficiency of fairway. In *International conference on algorithms and architectures for parallel processing* (pp. 366–375). https://doi.org/10.1007/978-3-319-11194-0_29